Accepted for publication in *Journal of Archaeological Science*
on 2nd July 2017

Repealing the Çatalhöyük extractive metallurgy:
The green, the fire and the 'slag'

Miljana Radivojević[1*], Thilo Rehren[2*], Shahina Farid[2], Ernst Pernicka[3] & Duygu Camurcuoğlu[4]

[1]McDonald Institute for Archaeological Research, University of Cambridge, Cambridge, UK; mr664@cam.ac.uk
[2]UCL Institute of Archaeology, London, UK; th.rehren@ucl.ac.uk, and College of Humanities and Social Sciences, HBKU, Doha, Qatar
[3]Curt Engelhorn Zentrum Archaeometrie, Mannheim, Germany
[4]Department of Conservation, The British Museum, London, UK

*corresponding authors

Abstract

The scholarly quest for the origins of metallurgy has focused on a broad region from the Balkans to Central Asia, with different scholars advocating a single origin and multiple origins, respectively. One particular find has been controversially discussed as the potentially earliest known example of copper smelting in western Eurasia, a copper 'slag' piece from the Late Neolithic to Chalcolithic site of Çatalhöyük in central Turkey. Here we present a new assessment of metal making at Çatalhöyük based on the re-analysis of minerals, mineral artefacts and high-temperature materials excavated in the 1960s by J. Mellaart and first analysed by Neuninger, Pittioni and Siegl in 1964. This paper focuses on copper-based minerals, the alleged piece of metallurgical slag, and copper metal beads, and their contextual relationship to each other. It is based on new microstructural, compositional and isotopic analyses, and a careful re-examination of the fieldwork documentation and analytical data related to the c. 8500 years old high-temperature debris at Çatalhöyük. We re-interpret the sample identified earlier as metallurgical slag as incidentally fired green pigment, which was originally deposited in a burial and later affected by a destructive fire that also charred the bones of the interred body. We also re-confirm the contemporary metal beads as made from native metal. Our results provide a new and conclusive explanation of the previously contentious find, and reposition Çatalhöyük in a new narrative of the multiple origins of metallurgy in the Old World.

Keywords: metallurgy, slag, copper minerals, pigments, Çatalhöyük, Anatolia

1. Introduction

Tracing the invention and spread of metallurgy is essential to understanding the relationship of this technology with the rise of social complexity, and ultimately, the economy of early civilisations during the transition from the Neolithic to the Metal Ages. The scholarly quest for the origins of metallurgy has focused on a broad region spanning the Balkans and Central Asia via Iran, known for the early use of metals. The site of Çatalhöyük, situated in the geographic centre of this broad region, represents a milestone in our understanding of past societies in Anatolia from as early as c. 7400 cal BC. The outstanding architectural and material legacy of this settlement has been attracting scholarly attention ever since its discovery, making it one of the best-studied prehistoric archaeological sites globally[1], with an exceptional number of specialists involved in building hypotheses on the evolution of prehistoric communities in this part of the world (Mickel, 2016).

Metallurgical activities at Çatalhöyük have long stimulated scholarly debates due to an unusually early date for a find that appeared to contain features of a metallurgical 'slag', set at c. 6500 cal BC (Neuninger et al., 1964; Mellaart, 1964; Cessford, 2005). This was based on analytical work conducted in the 1960s that identified this alleged evidence for copper smelting in an assemblage of archaeometallurgical materials dated around the mid-7th millennium cal BC. However, these materials have never been fully assessed within their archaeological and technological context. The argument that the Neolithic Çatalhöyük communities were possibly smelting metal has, since then, been discussed controversially in the literature, from ardent support (Hauptmann et al., 1993; Hauptmann, 2000) to plain acceptance (Strahm, 1984) and more cautious reception (Muhly, 1989; Pernicka, 1990; Craddock, 2001; Roberts et al., 2009; Birch et al., 2013) to open scepticism (Tylecote, 1976; Radivojević et al., 2010). Against such a backdrop, a full re-analysis of the original metallurgical 'slag' from Çatalhöyük was the only way to resolve this enigma.

Major progress has been made recently in our understanding of the beginnings of metallurgy in Eurasia, pushing the boundaries of what is known about the emergence of metal extraction, chronologically and spatially (e.g. Bourgarit, 2007; Radivojević, 2007; 2012; Radivojević et al., 2010; Radivojević et al., 2013; Murillo-Barroso and Montero-Ruíz, 2012; Leusch et al., 2014). Sensorial aspects of early technology in particular are growing in importance in these debates (for the Balkans see Radivojević and Rehren, 2016; Rehren et al., 2016). Some of these studies have revived the theory of multiple origins of metal extraction in Eurasia, as opposed to the long-standing argument for its single place of invention in the Near East (see Roberts et al., 2009). In this light, and drawing from the expertise gained from studying early Balkan metallurgy, our team revisited the Çatalhöyük metallurgical evidence. We were guided by the intention to investigate further the convergence hypothesis of metal invention (e.g. Renfrew, 1969; Radivojević, 2015), and to clarify the initial results from analyses by Neuninger et al. (1964).

[1] Full bibliography on http://www.catalhoyuk.com/research/bibliography

A total of 41 items from Mellaart's 'metallurgical finds' (polished blocks and glass containers with dozens of small fragments) from Çatalhöyük and Hacılar were available to us, including the material analysed by Neuninger et al. (1964) and Sperl (1990; 1991) (Fig. S1, Supplementary Materials). The results of our analyses of the key Çatalhöyük finds are presented below, as the basis for a revised hypothesis on how metallurgy developed in this Neolithic site in Anatolia, and beyond.

1.1. Early metal use in Eurasia

The view of early metallurgy as closely interwoven with, but distinct from stone bead manufacture has been presented elsewhere (Radivojević et al., 2010: 2784; Radivojević and Rehren, 2016); the latter going back well into the 11th millennium cal BC. By c. 6000 cal BC, the use of copper minerals and native copper had spread from Anatolia and the Levant across wide parts of Eurasia, including Syria (Golden, 2010), Transcaucasia (Kavtaradze, 1999), the Balkans (Glumac and Tringham, 1990; Radivojević and Kuzmanović-Cvetković, 2014; Radivojević, 2015), Iran (Pigott, 1999; Thornton, 2009; Helwing, 2013) and Pakistan (Kenoyer and Miller, 1999). The use of copper minerals has been strongly associated with their aesthetics, as has been observed in the use of 'greenstones' as inherently related to the rich symbolism of the green colour as a fertility charm (Bar-Yosef Mayer and Porat, 2008).

By the end of the 6th millennium cal BC, green copper minerals were transformed into copper metal by extraction, or *smelting*. Pernicka (1990) showed that low trace element concentrations (particularly cobalt and nickel) in copper metal indicate the use of native copper metal, based on hundreds of analyses of both objects and (native) copper from Anatolia and the Balkans (cf. Pernicka et al., 1993; Pernicka et al., 1997). The earliest securely documented evidence for copper smelting falls at around the transition of the 6th to the 5th millennium cal BC in the Balkans (Radivojević et al., 2010), and probably around that time in the Near East (Dougherty and Caldwell, 1966); the latter is still debated due to uncertainty concerning the archaeological and chronological evidence (cf. Frame, 2012; Thornton, 2014).

Thus, the copper 'slag' that Neuninger et al. (1964: 100-107) reported in Level VI at Çatalhöyük (c. 6500 cal BC, (Cessford, 2005: 69-70) as a potential evidence for local smelting of copper metal stands out as unusually early, by c. 1,500 years from the earliest recorded evidence elsewhere. Neuninger et al. (1964) reported that the sample in question has a limonitic core, akin to gossan, while the structure of the outer zone reflected high temperature treatment that resulted in the formation of a slag matrix with copper dross, delafossite and metal. Many scholars supported the idea of the intentional nature of a metal-making event this sample had been argued to demonstrate. While Muhly (1989) advocated that the 'slag' sample was melting (or refining) debris, Hauptmann et al. (1993) called it 'slagged ore'. Furthermore, Pernicka (1990), although acknowledging its confusing nature, interpreted this sample as a testimony of continuing heat treatment of different minerals, anticipating Craddock's (2001) interpretation that it sat at 'the verge of true smelting' at the site of Çatalhöyük.

Tylecote (1976), on the other hand, was more careful with accepting this sample as related to metallurgy, given its low content of iron, which would have been essential for a slag formation. Radivojević et al. (2010: 2776) have commented that the limited penetration of the outer slagged ('hot') zone into the core of the studied sample suggested a short-lived thermal impact, inconsistent with a mature process of early copper extraction. Here, we present a full analytical reassessment of this and other samples from the assemblage analysed by Neuninger, Pittioni and Sperl in the 1960s, in light of analytical advances made during the last half century.

1.2. Introduction to the site of Çatalhöyük

Mellaart conducted excavations at Çatalhöyük from 1961 to 1963 and in 1965. This period proved to be a 'Golden Age' for him as he had identified a Neolithic site that was hitherto unknown in central Anatolia. He had not only pushed back the boundary of the period of early farming and the domestication of cattle and plants west of the Fertile Crescent, but he also placed Çatalhöyük on the international stage of remarkable archaeological discoveries. He courted media to great effect and employed important scientific advances of the time to enhance his findings, such as ^{14}C dating, obsidian sourcing, and indeed archaeometallurgy.

The site of Çatalhöyük comprises two mounds, the East Neolithic Mound that dates from c. 7100 to 5950 cal BC (Bayliss et al., 2015; Marciniak et al., 2015) and the West, largely Chalcolithic or Late Neolithic Mound that ends at about 5600 cal BC, in a seemingly continuous occupation. The mounds formed through successively constructed houses; growing in height but also in extent as peripheral areas were expanded over. As each 'layer' of abutting buildings was exposed and excavated, Mellaart designated these neighbouring buildings into *Levels* that defined roughly contemporary neighbourhoods. Thus, at the top of the East mound, Level I represents the latest occupation horizon with Level XII towards the base of the mound; Level XII represents the earliest structures or middens excavated but not, necessarily, the earliest at the site. Although Mellaart distinguished between 'houses' and 'shrines' (see Supplementary Materials), excavations and research conducted under the directorship of Ian Hodder (1993 - current) reviewed these distinctions and led to a preference for a non-hierarchical classification of 'building', which will be used here.

Buildings were constructed independently on the footings of the old ones, and side-by-side. The walls of one building abutting the walls of its neighbouring building created tightly clustered buildings interspersed with open 'courtyard'/midden areas. Access into the buildings was via a roof opening. Internally, they followed a standard pattern of furnishing and arrangement but were differentiated through variances in size and detail. In general, ovens and hearths lay to the south coinciding with the roof entrance above. The western side was the usual place for storage features, and shallow platforms were arranged against other walls beneath which the dead were buried. Some buildings were embellished with wall art of geometric and figural paintings and moulded plaster relief sculpture.

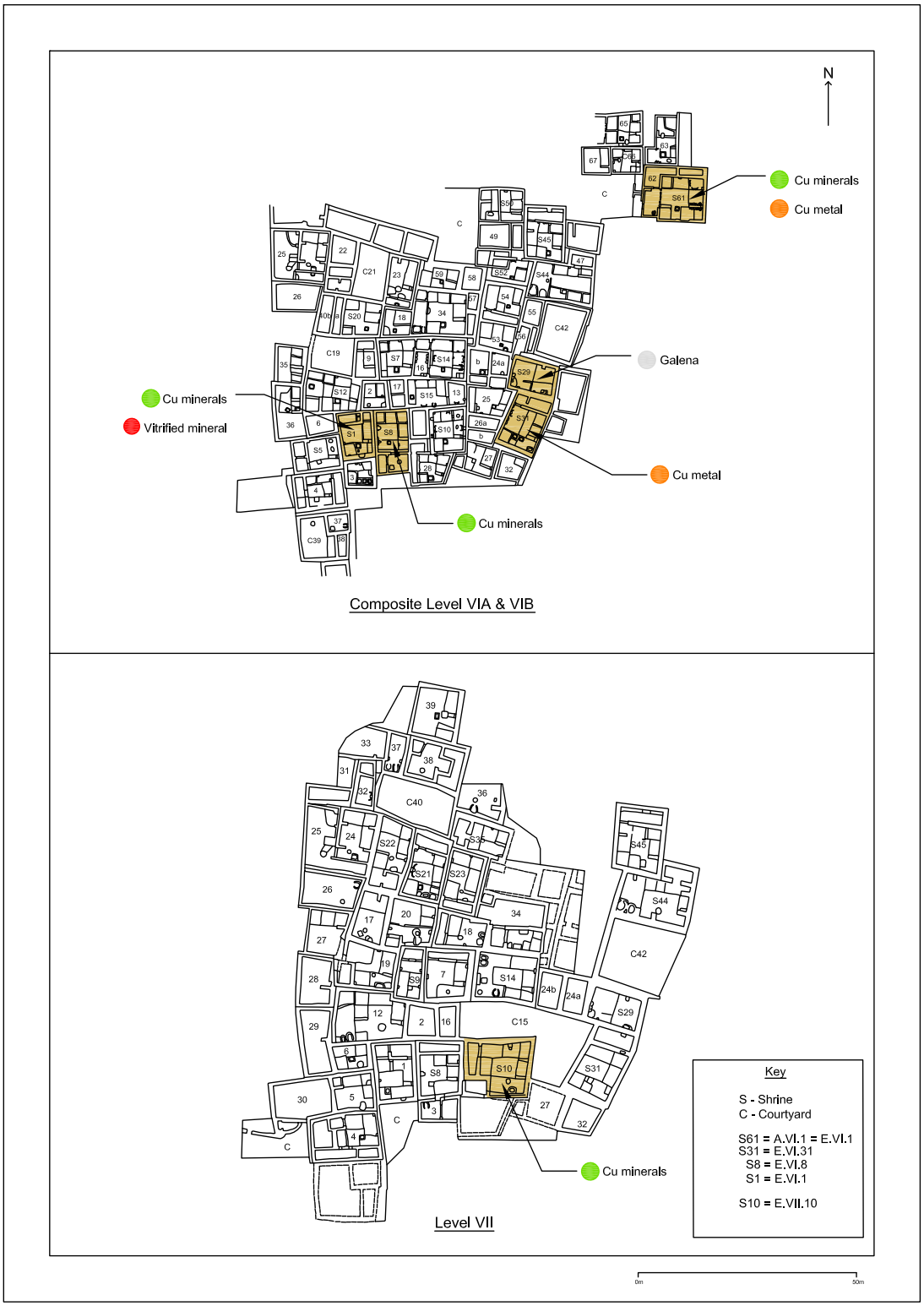

Figure 1: Floor plan for Levels VI (A&B) and VII with indicated building contexts and nature of studied samples.

1.3. Mellaart and metallurgy

It is difficult to assess Mellaart's excavation and sampling methodology as very little of the original archive survived a fire at his home in Istanbul in 1977 (J. Mellaart, pers. comm.). The available information mainly consists of the annual Anatolian Studies reports (Mellaart, 1962; 1963; 1964; 1966), his synthesis account (Mellaart, 1967) and some other published materials[2]. Beyond this, there is neither a comprehensive inventory of finds, nor any contextual records – that is the description of deposit type with lists of finds by deposit type or by building. Thus, the data available is very limited, despite detailed reports by artefact, which report on the material assemblage only (e.g. Bialor, 1962; Burnham, 1965; Mellaart, 1964: 73, 85, 92; Angel, 1971), rather than in conjunction with depositional events. Similarly, the 'Neolithic use of Metal' (Mellaart, 1964: 111) provides an overview of the material, the technology and the possible use of the objects; but lacking a comprehensive list of all metal finds and without the detailed description within depositional events, further interpretation is very limited. It is interesting to note, however, that whilst Mellaart was not an expert in the subject, it does, nevertheless, coincide with the report by Neuninger et al. (1964) and an article by Wertime (1964) at the end of that year, suggesting that Mellaart by this time had some specialist input. It is significant for the purpose of this paper that the renewed excavations, with ongoing field seasons from 1993 and careful sieving and flotation of excavated soil, revealed only very few further metal finds from the early layers. Most finds from the resumed excavation campaign recorded on site as metal were intrusive and of much later (Roman and Byzantine) date (Birch et al. 2013: 310). No further suspected metallurgical slag (or other metal production debris) has been identified to date.

The samples that Neuninger et al. (1964: 100-107) analysed came from six buildings only (Fig. 1, Table 1), from Levels VII and VI on the East Mound, and it is possible that some of the unprovenanced fragments, marked Level VI, could have come from the open midden areas that Mellaart called 'courtyards'. The six buildings, all defined by Mellaart as shrines (see Supplementary Materials for details on this designation), represent only 2 percent of the nearly 300 buildings recorded or excavated.

The only 'list' of metals is a published table (Mellaart, 1967: 81, Table 13) and shows a presence of metal artefacts identified as such by the excavator plotted against some shrines, together with wall paintings, plaster reliefs and materials like mirrors or cult statuettes. The table relevant to metals lists the 'Level' and 'Shrine number' in the y-axis, with types of motifs within the 'wall paintings' and 'plaster reliefs', and artefacts-types within 'burials' in the x-axis. In total, 58 'shrines' are listed spanning Levels II to IX with the presence of metal shown in 11 shrines. This table only shows a presence/absence marker and therefore gives no information on the form of the metal or any description that would inform the veracity of depositional intent. Significantly, as will be shown in the analyses below, Mellaart apparently did not distinguish minerals from metals (see Table 2). Throughout his reports, Mellaart's 'metallurgical' terminology included copper, ores, slag, lead, galena and

[2] http://www.catalhoyuk.com/research/bibliography

lignite; however, none of these differentiations are seen in the presence / absence of 'metal' finds in Table 2. The inconsistency of such an approach is also detected in selective labelling of copper minerals as 'metals', as seen for instance in the building E.VIB.8[3], where two copper minerals were marked as 'metals' in the Mellaart's list (Table 2). We therefore doubt that finds from levels IX and VII were metals in a true material sense of this term, but rather any type of material Mellaart held as related to the idea of metallurgy, such as various colourful minerals. In the light of these inconsistencies in reporting truly metallic finds, we believe that the samples that reached Neuninger et al. were all metal and metal-related samples from Mellaart's excavations. An alternative hypothesis that Mellaart did not send all metal-related samples to Austria could be valid; unfortunately there is no information of whatever the remaining samples are or where they might be located.

Noteworthy is in this regard Mellaart's appreciation for the shared aesthetic appeal of minerals and metals. In his 1964 report he writes: "*The discovery of metal ores or native copper at this early date in Anatolia is perhaps not so surprising. The traders and prospectors of Çatal Hüyük roamed far and wide in their search for raw materials, colourful stones, fossils, concretions, etc., and the brilliantly coloured copper ores-a bright blue azurite and the green malachite (?) which ground up into a powder were used in the burial rites in Levels VI and VII - as well as the fine red and heavy native copper, are materials (like lead (galena), haematite, cinnabar, apatite, etc.) conspicuous by their colour and weight, sought after and highly prized*" (Mellaart, 1964: 114).

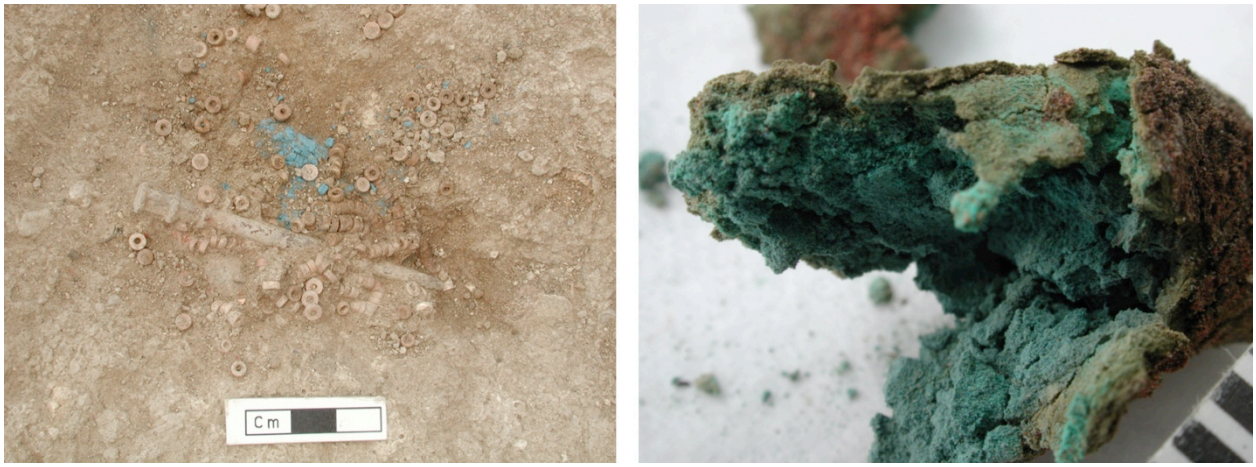

Figure 2: left) Blue pigments (azurite) scattered as lumps in Burial 1202 in Çatalhöyük (campaign 2003). The distribution might have been an indication of deposition as either loose lumps or in a (skin or fabric) pouch that had decayed (courtesy of the Çatalhöyük Research Project); right) Green pigment (malachite) from Burial 757 (campaign 2001) in Çatalhöyük, discovered as a lump that seems to have preserved the shape of the original organic carrier (fabric or skin pouch). Note the crumbly nature of recovered pigment and soil coating (courtesy of the Çatalhöyük Research Project).

[3] The numbering convention is as follows: alphabetical prefix indicates the spatial area of excavation (areas A, E & F), the Roman numeral infix denotes the level and the numerical suffix represents the building number.

Significantly, Mellaart (1964: 92) describes the use of metal-based pigments in 'burial rites'. He (1961: 56) claimed that "*green paint was found on three burials in Levels VI and VII. In one case, a male (?), it covered the bones; in another, female, it had been applied to the 'eyebrows' on the skull*". In the same article, he also reported that blue and green powdered azurite and apatite was found in lumps near the skulls of the skeletal remains, and "*red and green paint was found in lumps or ready for use in the shells of freshwater mussels*". Powdered azurite and malachite were also found in renewed excavations of Çatalhöyük in shapes reminiscent of a small pouch, or scattered as lumps (see examples in Fig. 2, Table S3 in Supplementary Materials), together with miniature bone spatulas, and associated mainly with female and infant burials (Camurcuoğlu, 2015). Detailed microscopic analyses by Camurcuoğlu (2015) revealed that these pigments were coated with clay and iron oxide particles, while angular and sub-angular shapes of either green or blue phases indicated that the pigments might have been hand-ground. The startling predominant evidence of blue-only or green-only phases present in blue and green pigments respectively imply the importance of colour 'purity' that was probably highly sought after and that might have had a particular symbolic meaning. The latter assumption is highlighted by the fact that no blue or green pigments were identified in the wall paintings or any other activity in this site, which leaves us with assumption of their specific ritual role as burial offerings. The context and the results of analyses of Çatalhöyük green and blue powders led Camurcuoğlu (2015) to recognise these as the earliest documented use of malachite and azurite as pigments, anywhere. Red (ochre or cinnabar) is less commonly found in lumps, however, it is also found in powder form staining small containers of shell or stone, or 'painted' onto bones (Mellaart, 1963: 50; Mellaart, 1964: 93; Mellaart, 1966: 183; Angel, 1971).

1.4. Context evaluation of samples analysed by Neuninger et al.

Table 1 provides the list of samples that were excavated by J. Mellaart, sent to H. Neuninger for analysis and now form the core of this study. Only samples CHM 11 from Grave 5, building E.VI.1 and galena from building E.VI.29 have been published thus far (Neuninger et al., 1964; Sperl, 1990; 1991). Neuninger et al. (1964: 99, Tab. 1) mention that their team conducted compositional analyses of a further four copper metal (bead) samples, however, no actual field labels were provided, apart from analytical numbers (3862-3865). Out of forty-one samples in total, thirty-six are studied here (labelled CHM and a related number). We received the entire assemblage with an accompanying table designating the context of all finds, and boxes/sections that they belonged to (Table 1, Fig. S1 in Supplementary Materials).

The chronologically earliest samples (CHM 5; CHM 6; CHM 7; CHM 8) are copper-based minerals from a single building *E.VII.10* at Level VII, where out of c. forty-four buildings exposed only thirteen were excavated with their complete occupation sequence. This building was revealed in 1963 (Mellaart, 1964), consisting of two spaces (Fig. 1). The larger, eastern space had platforms arranged along three walls, those on the eastern side being separated by benches. A sunken area was defined to the south where the oven was set against the wall

towards the eastern end with a circular hearth in front. A crawl-hole at the northern end of the west wall led to a narrow western space, which was excavated by the Hodder team (Farid, 2007). The building is recorded as containing animals sunk in relief and animal installations (Mellaart, 1964; 1967). Numerous burials were excavated in the 1965 season, two of which were noteworthy female ochre burials (Angel, 1971). The head of one was reported as being '*entirely covered in red ochre and cowrie shells had dropped out of the eye sockets*' (Mellaart, 1966: 183). Whilst there is no indication of any recovered metal objects from this building (see Table 2), samples CHM 5-8 have labels describing them as '*ore lump from House E.VII.10*' (CHM 5-6) and as '*copper lumps with soil from House E.VII.10*' (CHM 7-8). Neither label specifies the samples as deriving from *in situ* deposits and indeed, the latter description could imply that CHM 7 and CHM 8 were identified as different from the ore lumps CHM 5 and CHM 6 (Fig. 3), or, alternatively, that they were collected from the infill of the building where a secondary context would not be too far from their primary phase.

The overlying Level VI horizon of buildings was by far the largest exposed comprising c. forty-nine excavated buildings, from which five buildings yielded materials for our study (Tables 1 and 2). At Level VI Mellaart encountered stratigraphic problems such that he reports (Mellaart, 1964: 40), arguing that it was necessary to divide Level VI into Levels VIA (Late) and VIB (Early). Any of these numbering conventions (Level VI, Level VIA, Level VIB) may be encountered in relation to this paper, which have not been changed from the initial numbering in order not to lose original citations. However, for the purpose of this paper all have been stratigraphically validated as Level VI[4]. It is also at this level that Mellaart reports the end of Level VI as a '*violent destruction*' (Mellaart, 1964: 115). He (Mellaart, 1964: 85) also notes: "*The conflagration which put an end to Level VI A was of such intensity that the heat of the burning buildings above penetrated to the depth of about 3 feet or more below the floor level of the buildings, carbonizing bodies and burial gifts alike and preventing all further bacterial decay".*

Current discourse on burnt buildings from the renewed excavations centre around the debate of deliberate versus accidental burning of buildings (Cessford and Near, 2005; Twiss et al., 2008). The forensic fire examination of these burnt buildings conducted by Harrison et al. (2013) identified a range of mechanisms by which buildings burned at Çatalhöyük involving 'compartment' and 'combustion' fires, which depend on fuel load and thermal characteristics. Experimental work conducted to assess the ability to raise subsurface deposits to such temperatures that fully charred skeletal remains and, in some cases carbonised brain tissue, was undertaken on porcine brain tissue. It demonstrated that a temperature of c. 300 °C must be maintained over about a two-hour period for the brain tissue to be carbonised but to char bone 30 kg of timber was required to fuel a fire over an eight-hour period. The conclusion is that the duration of burning was the dominant variable in producing carbonisation of bone rather than the peak temperature achieved.

[4] E.VI.29 & E.VI.31 were both reassigned to Level VII later in the excavations by Mellaart, although he later kept changing his mind on the assignment of these buildings to Levels VIa, VIb or VII. For the purpose of this report, we keep the original assignment to Level VI, which also matches the labels of the studied samples.

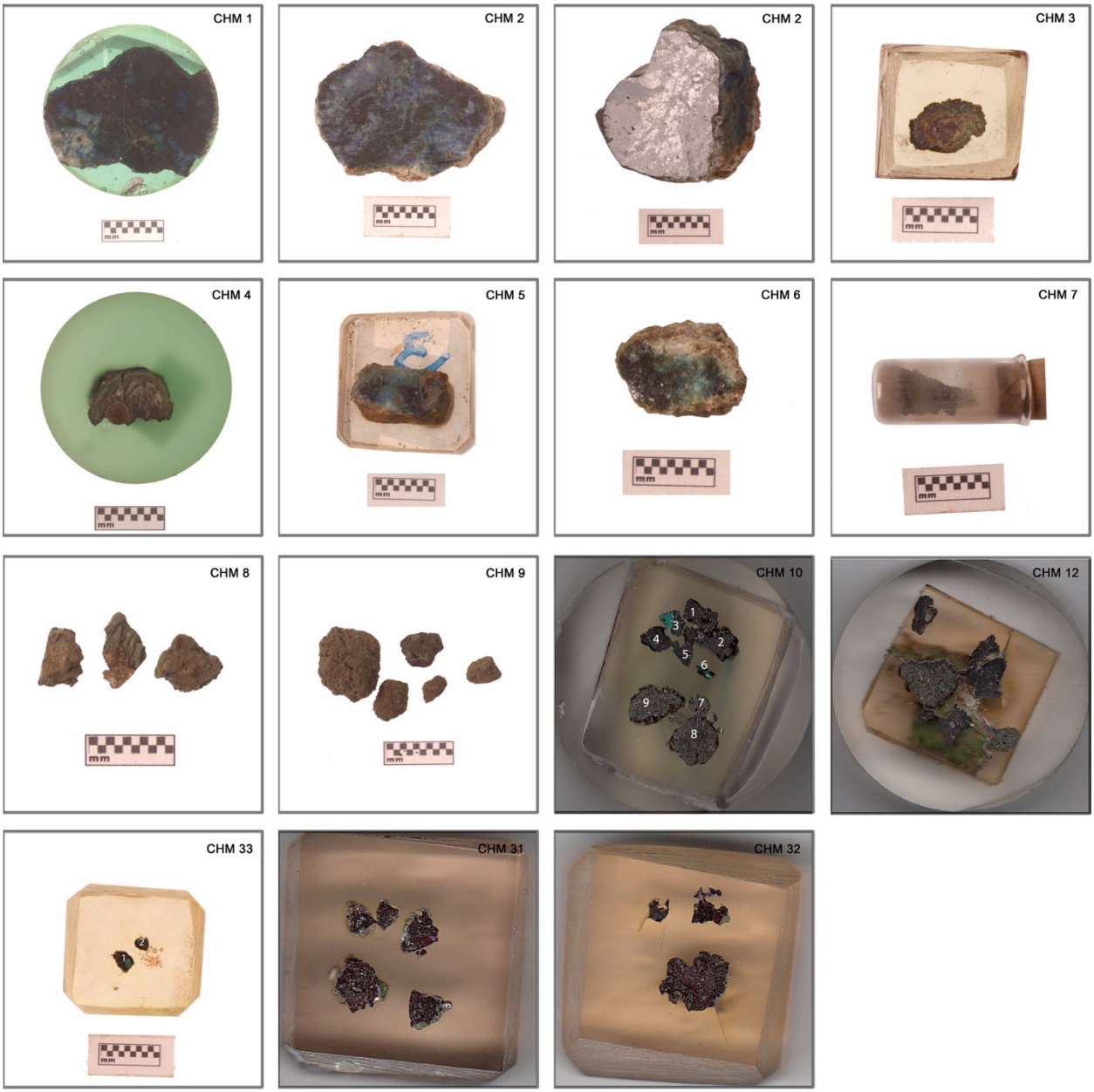

Figure 3. Copper-based minerals and haematite samples. Clockwise: CHM 1, CHM 2 polished, CHM 2 unpolished, CHM 3, CHM 4, CHM 5, CHM 6, CHM 7, CHM 8, CHM 9, CHM 10, CHM 12, CHM 33, CHM 31 and CHM 32.

Building A.VI.1, which yielded samples CHM 1-2 and CHM 13-16, was excavated in 1962 (Mellaart, 1963). Later, it is renumbered on plans as '*shrine 61*' in both Levels VI A and VI B (Mellaart, 1964: Fig. 1, 2). The building is shown as a large space with platforms along the north, east and south walls (See S61 in Fig. 1). Along the southern wall was the mark of the ladder and an oven set into the wall, with a hearth in front. A second space seems to have been entered through a 'post-and-plaster' screen along the western side. It was embellished with red panels and red-painted grooves. There were two 'bull pillars' and a bench with seven pairs of cattle horns

(Mellaart, 1963; 1967). A total of 13 skeletons were excavated from this building (Mellaart, 1967: 205). Mellaart (1964: 95) reports that *"women as well as men in Shrine A.VI.1 wore copper finger-rings"* (see Tables 1 and 2), which is the only suggestion that rings were found on more than one skeleton in this shrine.

Other artefacts in Shrine 61 included an obsidian lance and arrowheads, two pots and numerous food remains in the anteroom where the floor was covered in matting, as well as the carbonised remains of two circular baskets, a wooden dish with handles, two polished stone maceheads and a painted clay figurine (Mellaart, 1963; 1966; 1967). This was described as "*massive remains of a very large shrine of Level VI (A VI. I), which had been destroyed in a tremendous conflagration*" (Mellaart, 1963: 50). Such an interpretation was probably based on the presence of two large carbonised roof beams that were recovered in the debris of the main room. Samples CHM 1 and 2 are simply labelled as '*ore lump from Shine A.VI.1*' (see Table 1). Samples CHM 13 to 16, however, are labelled as '*beads from the grave in the northern corner of Shrine A.VI.1*'. These 'beads', whilst positively associated with a primary context in this building are not, however, associated to a specific grave or platform in the northeast corner. We believe that these beads are the only metal samples available for study from the context of this building, since we could not identify any of the 'copper finger-rings' Mellaart (1964: 95) documented, not even in fragmented state (see below Fig. 7).

Shrine E.VI.1 is the building from which samples CHM 9-12 originate. It was excavated in 1961 (Mellaart, 1962) as a three 'room' building. A small northwestern room had two storage features along its east wall and was accessed from a crawl-hole at its western end. The larger, central, space had platforms along the east wall. A recess in the southern space marked the place of an oven with a hearth in front and a possible large storage bin in the southeastern corner, which Mellaart generally described as 'plaster bins for grain' (Mellaart, 1963: 45). Several wall paintings of symbols, kilim/textile patterns, and simple patterns were revealed. There were also reliefs of a goddess, a female breast, a possible animal-head and horns set along the edge of a bench (Mellaart, 1967). Thirty skeletons were recorded as being excavated (Mellaart, 1964) from this building, although only 25 were studied by Angel (1971), of which one male and four female skeletons were carbonised black. In addition, fragments of charred textile were recovered and carbonised cloth found inside the skull of one (Burnham, 1965). These are the only references corroborating that the building had '*been replastered after a fire*' (Mellaart, 1963: 59). A necklace of fine limestone and carved serpentine beads were found with a female skeleton and a bone belt-set from another burial. Other artefacts from within the house included pottery, a double-pointed 'willow-leaf" obsidian point, eight other projectile points, a lancehead (Bialor, 1962), two stamp seals and a wooden box with a lid (Mellaart, 1964; 1967). Samples CHM 9 to 12 are labelled as originating from '*Grave 5 from the central platform, House E.VI.1*'. As there is only one central platform in this building, against the eastern wall, it is with some certainty that we can assign Grave 5 to that platform, but no further information is available on the number of graves that cut the platform or the stratigraphic location of Grave 5 within the platform. The same is therefore valid for samples CHM 9 to 12; we do not know which buried individual were they associated with

except that these samples were reported as a potential burial offering. We also do not know if the individual buried in Grave 5 was carbonised black after a fire, although we are aware that the fire reached up to c. 90 cm (3 feet) deep 'carbonising bodies and the burial gifts alike' (Mellaart, 1964: 85). Sample CHM 11 was identified as copper slag by Neuninger et al. (1964), prompting Mellaart (1964: 114) to suggest that the process of copper smelting might have been known at the time.

The neighbouring building to the east, *E.VI.8*, was excavated in 1962 (Mellaart, 1963) and at the end destroyed by fire (Mellaart, 1964: 40). The largest of three rooms in this building led into to a southeastern room through a crawl-hole, which led in turn via another crawl-hole to a southwestern room. The southeastern area appears to have contained a central circular hearth or basin as well as a sub-rectangular hearth in the southwest corner. The larger room had platforms along its north and east walls, with a bench between the two most southerly. Mellaart (1967) reported a sunken animal relief, a goddess, an animal-head, bucrania, and breast reliefs, as well as a pattern of hands and a red 'net' design on the east wall. Fifteen skeletons were excavated, four of which were carbonised black (Angel, 1971). Mellaart (1963: 95) also mentions a burial whose complete corpse was covered by red ochre. A fragment of charred textile was recovered (Burnham, 1965: 172), together with two greenstone celts and two ceramic pendants from female burials. Also, a recovered assemblage includes a wooden spoon from a burial, an obsidian pendant, lignite beads and a red sandstone spouted dish. The label for samples CHM 3 and 4 describes these as '*copper lumps from grave 2 at E.VI.8*' but again, we do not have further contextual information on which platform 'grave 2' was located.

Separated by two buildings, *E.VI.31* was excavated in 1962 (Mellaart, 1963). It consisted of a large space with two small spaces entered by crawl-holes to the north (see Fig. 1). The larger space had two platforms along the east wall ending in a bench and a possible platform against the west wall. To the south lay an oven with two hearths and a platform in the southwest corner. There was also an installation of two superimposed bull's heads between two plastered posts with other features above (Mellaart, 1963). The presence of burials was indicated only on Table 13 (Mellaart, 1967: 81), and therefore the number is unknown. Mellaart (1963) records that the building was destroyed by fire but provides no further information. The samples CHM 29 and 30 from this building are labelled and described as '*two beads from a burial, Shrine E.VI.31*', and as such it is not possible to identify which of the four possible platforms this 'burial' may have been located in.

Neighbouring to the north, *E.VI.29* was also excavated in 1962 (Mellaart, 1963). This was a single space demarcated into four with a possible sunken southeast quadrant where the oven was located. A platform possibly lay to the northeast with a series of features in the southwest corner. It may have had a relief on its western wall. Ten skeletons were studied from this building (Angel, 1971), and a white marble dish and flint dagger were recorded as being found with a male burial. Another male burial was found with a bone or horn scoop, and a bone belt-set was found from another burial. There is no mention of a fire or burning and the occurrence of 'metal' from this building is recorded on Table 13 (Mellaart, 1967: 81) only. The label *'lead from Grave*

E.VI.29' accompanies samples CHM 17 to 28 (Table 1). The location of the grave within this building is, again, unknown. Although initially identified as 'lead metal', they were since shown as made from cerussite and galena, minerals rich in lead, but not lead metal (Sperl, 1990).

A further five samples (CHM 31 to 35, haematite and copper-based minerals), CHM 36 (obsidian) and CHM 37 (a 'green' sample) have simply been labelled as coming from '*Level VI*', and as such are a group of un-provenanced samples albeit but all being from Level VI and therefore relatively significant for this study.

A further eight buildings are indicated in Table 13 (Mellaart 1963: 81) as having yielded 'metal' but from which no material was exported for analysis by Neuninger et al. Chronologically, the earliest mention of 'metal' comes from Level IX, from where in *Shrine E.IX.1* Mellaart records that a female was covered in red ochre, cinnabar was applied to her skull and with her '*were several necklaces and some copper and lead beads, the earliest found on the site*' (Mellaart, 1964: 93; 1967: 207). At Level VI a burial of an adult woman and child from building *E.VI.25* is described as containing patches of carbonised textile, including '*many fragments of a string-skirt the ends of which appear to have been encased in thin copper tutuli to weight it down*' (Mellaart, 1963: 101; 1967: 219). 'Metal' from another Level VI building is reported from *E.VI.5,* from which Angel (1971: 79) studied 19 skeletons. One male and three females were carbonised black. Many of the bones were wrapped in textile of various weaves and fineness, and tied into bundles with tapes. One skull was wrapped in textile soaked in red ochre. No pottery was found in this pit, but two polished bone pendants, a small copper roll, and a number of carbonised wooden vessels were recovered (Helbaek, 1963). Finally, the presence of metal from the following six buildings is shown in Mellaart's Table 13 only (Mellaart, 1967: 81): *E.VII.35*, *E.VIB.10*, *E.VIB.12*, *E.IV.8* and the chronologically latest, in *A.II.1*.

Other references to 'metals' emerge throughout Mellaart's reports and publications in general discourse and overview of technology, craftsmanship and ritual. He asserts that the use of two metals, copper and lead was familiar at least as early as Level IX, and that "*lead beads and pendants, especially in Levels VII and VI, and copper was used for beads, pendants, finger-rings, small tutuli which enclosed the lower ends of string skirts (in VI), small tubes (VII) and possibly pins and awls in Level II."* However, it was the occurrence of a *"supposed lump of copper ore from House E VI A, that proved to be not ore, but copper slag, suggesting that the process of smelting may already have been known, by the middle of the 7th millennium, but further analyses are required to establish how usual this was*" (Mellaart, 1964: 111), that is finally being addressed in this paper.

Whilst from today's perspective the reporting of the 'metal' finds is limited and frustrating, for the time when Mellaart was conducting his excavations, the discovery was practically a unique one, which he dealt with within the recording and analytical tools available at the time. Due to the absence of detailed locational or contextual data it is not possible to ascertain veracity of the exact find spots for all of the re-analysed metal samples; however, for the first time we were able to gather all relevant information for their context in the text above.

The most recent analyses of three Neolithic copper beads from the East Mound by Birch et al. (2013) further attest the presence of copper metal artefacts on this site from levels II to VI, with a greater contextual precision (see Table S4 in Supplementary Materials). Five pieces of metal were analysed, belonging to three distinctive groups of fragmented beads and rings from both burial and infill/dump deposit layers. They were found to consist of hammered and annealed pure copper metal, rolled up to form beads which contained only traces of Ag (up to c. 300 ppm) and As (up to c. 90 ppm) in two ring fragments (Birch et al., 2013: 309, Tab. 17.2). Given the low concentrations of trace elements such as cobalt, nickel, antimony and lead in these objects, it is argued that they were most likely made from native copper (Birch et al., 2013; cf. Pernicka et al., 1997). The working evidence corroborates the findings of Neuninger et al. (1964), matching the common metal working practice in Anatolia from as early as the 8th mill cal BC (e.g. Stech, 1990; Maddin et al., 1991).

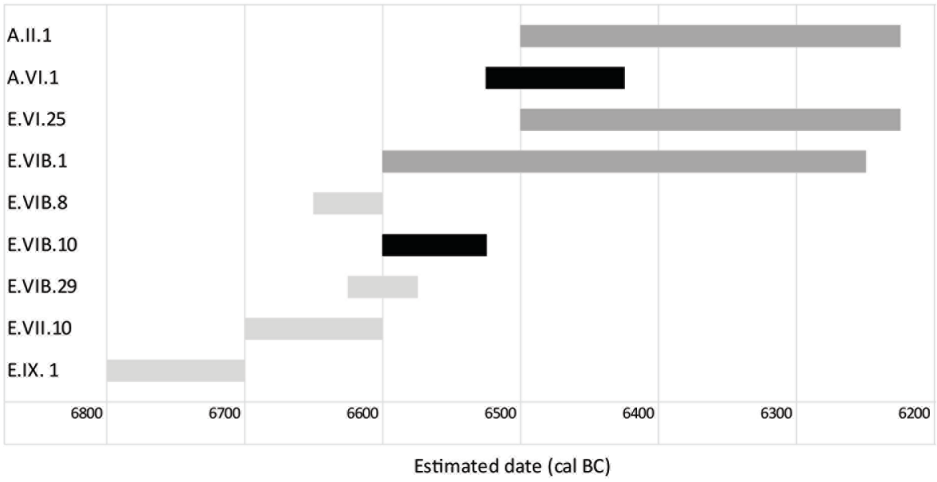

Figure 4: Estimated dates for buildings that yielded metal-related finds (black: derived from wiggle-match of floating tree-ring sequence; dark grey: calibrated radiocarbon dates; light grey: derived from interim chronological model for ongoing dating project).

The dating of the site in the 1960s is based on radiocarbon measurements of 27 samples that spanned buildings from all levels, of which eight were from buildings that contained metallurgical finds. These radiocarbon dates have been combined with Mellaart's phasing scheme of successive building levels in a Bayesian chronological model, which estimates the dates of those levels (Cessford, 2005: 66-79). The stratigraphic integrity of these levels, however, is under review by a current programme of radiocarbon dating and Bayesian modeling. This is attempting to combine the stratigraphical sequence of buildings and open areas with a large series of carefully selected radiocarbon dates, from both the renewed excavations and the 1960s archive. Both the radiocarbon dating and stratigraphic programmes are on-going and only partially reported (Bayliss et al., 2015; Marciniak et al., 2015); nevertheless, this project has thus far obtained radiocarbon dates for four buildings from which Mellaart reports metallurgical finds and has stratigraphic evidence allowing seven to be included in the Bayesian

chronological model (for a detailed account see Supplementary Materials). This model provides a more detailed account of chronology of Level VI in indicating that it does not form a concentrated chronological horizon (Fig. 4). A.VI.1, for example, appears to be about a century later than E.VIB.8 and E.VIB.29, and overall buildings assigned to Level VI appear to fall anywhere between the 67th and 64th centuries cal BC. On current evidence, it appears that metal and metal-related finds occur at Çatalhöyük across much of the seventh millennium cal BC (A. Bayliss, pers. comm.).

2. Materials and Methods

2.1. Characterisation of minerals and metal finds in Çatalhöyük

The assemblage of samples received consists of 41 items in total, 36 from Çatalhöyük, 4 from Hacılar and one that turned out to be a modern slag piece (see Supplementary Materials for further detail). It includes copper-based minerals, crumbs of copper-based 'slag', galena minerals, galena and copper metal beads, a piece of obsidian, and a green stained piece of bone (?). We concentrate below only on copper-based minerals, copper metal beads and the copper 'slag'.

Copper-based minerals include CHM 1 to 10, 12 and 33 (Table 1, Fig. 3). Their macroscopic appearance varies in relation to the context. The 'free' building finds (CHM 1, 2, 5 and 6) are of similar appearances both as free and as mounted samples: they are lumps of minerals 1-2 cm in length, with blue and green streaks coming through the pale surface of amorphous samples, while the polished surfaces expose a mix of dark body with green/blue components. Samples CHM 7 to 10 and 12 come from either a domestic (E.VII.10) or funerary context (E.VI.1), and although originating from different levels, they share a similar appearance, being coated with soil, granular and crumbly green materials a few millimetres wide. Samples CHM 3 and 4 come from a burial, and are up to 1 cm long lumps of green and red components visible on the polished surface. We studied in more detail samples CHM 1, 3 to 5, 9, 10, 12 and 33. Resin blocks with samples CHM 9, 10, 12 and 33 consist of several similar-looking items (ranging from 2 to 9), which we refer to as 'locations' in our analyses (see Fig 3).

The 'slag' sample CHM 11 belongs to a batch of items from the central platform, Grave 5, building E.VI.1, which consists of a dozen non-magnetic crumbly copper-based minerals (here embedded in blocks CHM 9, 10 and 12) in addition to this one. Sample CHM 11 consists of 15 smaller items marked as 'locations' (Fig. 5) in our microstructural and compositional analyses, giving each item a unique number. According to the images available to us from the previous study, we believe that CHM 11 is the sample Neuninger et al. (1964: 100)

identified as ‘slag debris with molten copper oxide’. Neuninger and collaborators (1964: 99, Tab. 1) identified traces of Ni, Zn, As and Co in the mentioned sample, while Sperl in 1997[5] identifies antimony in it as well.

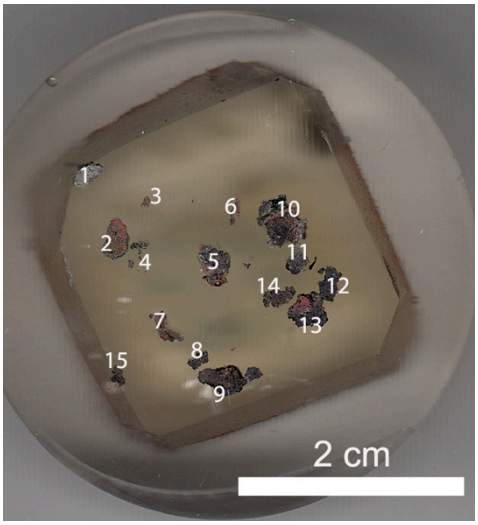

Figure 5. Copper ‘slag’ sample CHM 11 with marked ‘locations’

Copper metal beads (CHM 13 to 16, 29, 30, 34 and 35) originate from two burial contexts in buildings A.VI.1 and E.VI.31 respectively, while CHM 34 and CHM 35 come from the soil of Level VI. The richest collection of metal beads comes from the burial in building A.VI.1; we estimate there are c. 53 copper metal beads, although the exact number is difficult to assess due to the heavy corrosion and fragmentation of these artefacts (Fig. 6). The beads are either of a short, circular shape, or tubular, common for the period and with a long history in the region of origin (e.g. Maddin et al., 1999). We studied in more detail samples CHM 14, 15 (joint block with CHM 30), CHM 34 and 35, while CHM 13 and 16 were analysed for provenance only (see Table S2 in Supplementary Materials). The published analyses of four of these metal beads identified high purity copper metal with traces of Ag (Neuninger et al., 1964: 99, Tab. 1) without specifying which samples these were. In addition to the described set of samples, we also analysed two blocks with several samples of mineral haematite (CHM 31 and 32, Fig. 3), which are not further considered here. Also, the analyses of galena minerals and beads will be presented separately elsewhere.

[5] We found this information as a note on what appears to be a poster presentation by G. Sperl, titled “New Research on the Beginnings of Metallurgy at Çatalhöyük, Turkey (7th mill BC)”, presented at Harvard University in 1997.

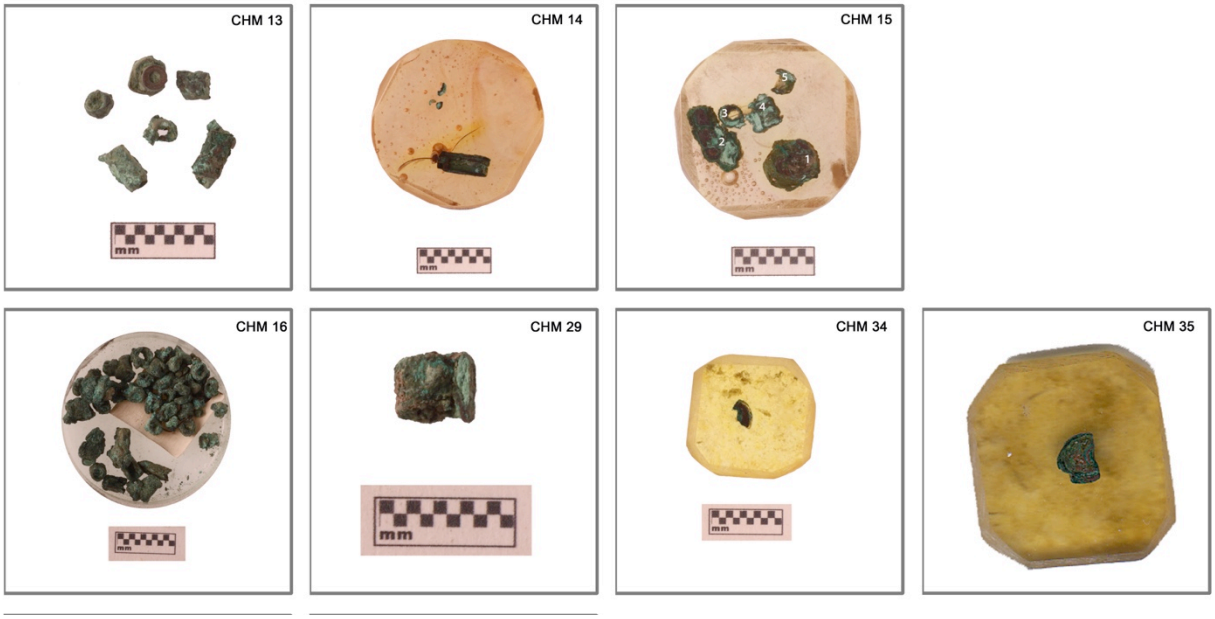

Figure 6: Copper metal. Clockwise: CHM 13, CHM 14, CHM 15 & CHM 30 (CHM 30: loc. 1 and CHM 15: loc. 2-5), CHM 16, CHM 29, CHM 34, CHM 35.

2.2. Methods

In total, we analysed 19 samples for microstructure, chemical composition and possible provenance (as indicated in Tables 1 and S2), out of the assemblage consisting of 36 samples excavated by J. Mellaart in Çatalhöyük in the 1960s, including some that had already been analysed by Neuninger et al. (1964) and Sperl (1990). Of these 19, 18 belong to Neolithic Çatalhöyük, while one (CHM 27) is a modern slag sample that might have ended up accidentally in this collection. A further five samples (CHM 6, 7, 8 and 29) were only characterised macroscopically. Table S2 indicates that we have also conducted analytical work on galena samples, which we will report in a separate article.

In total, we analysed all existing polished blocks (16 samples were already mounted in 15 blocks that were re-cast and re-polished by us), together with a freshly made block (CHM 9) for microstructure and composition with OM (Optical Microscope) and SEM-EDS (Scanning Electron Microscope with Energy Dispersive Spectrometer) at the Wolfson Archaeological Science Laboratories, UCL Institute of Archaeology, London. Provenance and trace element analyses were conducted with MC-ICP-MS (Multi-Collector Inductively-Coupled Plasma Mass Spectrometer) and LA-ICP-MS (Laser Ablation Inductively-Coupled Plasma Mass Spectrometer) at the Curt-Engelhorn Centre for Archaeometry in Mannheim, Germany (see Supplementary Materials).

Copper-based minerals studied here are recognised as only potentially representing copper ores, which is why we kept the neutral term ‘mineral’. We see *ore* as a culturally and economically defined term referring to agglomerations of minerals from which the extraction of one or more metals is seen as a profitable action

(Rehren, 1997; Rapp, 2009). The importance of this distinction of copper minerals in the context of potential pyrometallurgical activities has already been recognised by Muhly (1989), who noted that the presence of malachite at an archaeological site has little to do with copper metallurgy, as much as the presence of haematite in a cave painting context has nothing to do with iron metallurgy. The only potential evidence of extractive metallurgy, CHM 11, we termed 'slag' with quotation marks because we question here the nature of its creation.

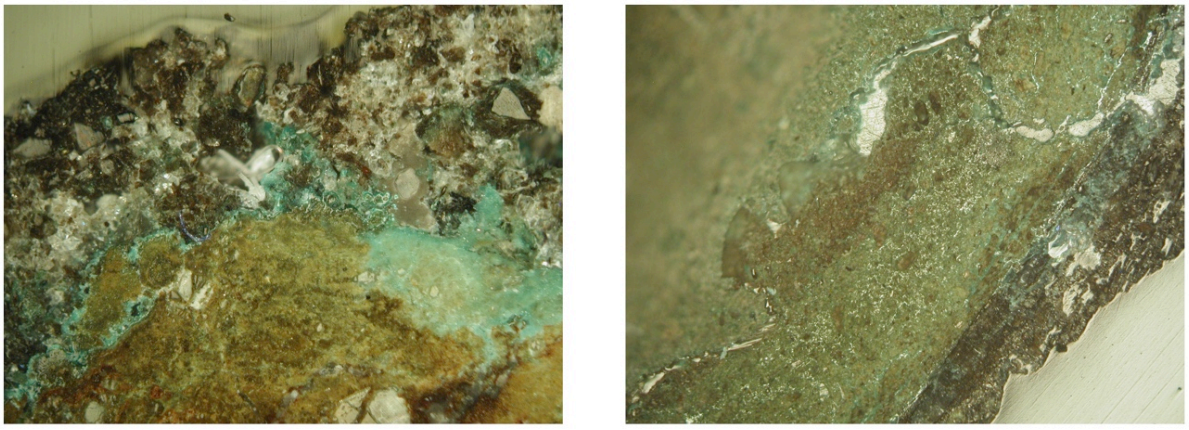

Figure 7: left) Photomicrograph of CHM 3 under cross polarised light (magnification 50x, width 3.2mm). Note the green matrix rich in copper content; right) Photomicrograph of CHM 4 under cross polarised light (magnification 50x, width 3.2 mm).

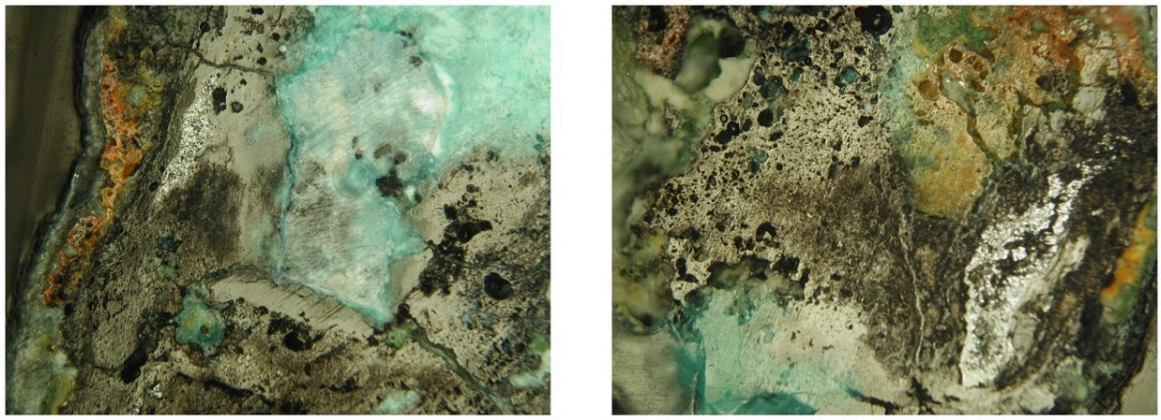

Figure 8: left) Photomicrograph of CHM 33 (location 1) under cross polarised light (magnification 100x, width 1.6mm); right) Photomicrograph of CHM 33 (location 2) under cross polarised light (magnification 100x, width 1.6mm). Note green copper-rich phases in both locations in this sample.

3. Results

3.1. Copper-based minerals

The copper-based minerals form two distinctive groups: oxide (CHM 3, 4, 9, 10, 12 and 33) and sulfide (CHM 1 and 5) minerals. Macroscopically, they differ in texture: while oxide minerals are small-sized and crumbly, the sulfide examples are solid lumps of ore (Fig. 3). The oxide minerals contain a predominant copper-rich phase (see Figures 7-10) with only traces of zinc found in CHM 9 and 10 (Table 3). Besides the copper-rich matrix, both CHM 9 and CHM 10 contain phases with various antimony and antimony and arsenic readings respectively (Table 4). These phases contain lead and various levels of Cu, pointing at the composition of minerals that belong to the lead-bearing arsenates and vanadates (Dana and Ford, 1922).

The composition of the Sb-bearing mineral phase in CHM 9 is close to valentinite (Sb_2O_3), however the calcium and lead components classify it as more likely as a mineral of romeite group, or a similar mineral that belongs to the family of antimonates, arsenates and vanadates. This could have originated as a weathering product of primary stibnite (Sb_2S_3), with lead and calcium precipitating from the surrounding geological environment. Stibnite is usually accompanied with various other antimony-bearing minerals produced by its alteration, and significantly for this context, occurs with sphalerite, galena or cinnabar (Dana and Ford, 1922: 359); this could explain the presence of lead in the phase observed here. The common denominator for these secondary minerals is the antimony content, while their outer appearance varies from pale yellow to olive green tones.

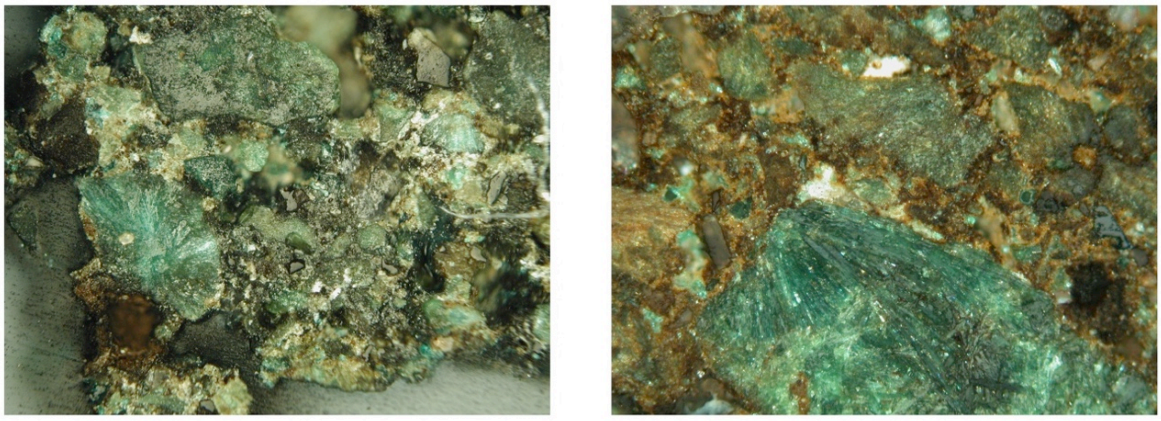

Figure 9: left) Photomicrograph of CHM 9 under cross polarised light (magnification 100x, width 1.6mm). The green phases are rich in copper, while white/bright ones are antimony oxides; right) Photomicrograph of CHM 10 (location 2) under cross polarised light (magnification 100x, width 1 mm). The white/bright phases have significant levels of Sb, As, Pb and Cu. Both samples appear coated in soil and rich in iron oxides (orange/red).

A macroscopically similar mineral phase in CHM 10 reveals significant readings of antimony, arsenic and lead besides copper, and is a potential member of the same mineral group as the similar phase in CHM 9, romeite, with variations including cuproromeite (with Cu), oxyplumboromeite (with Pb) and oxycalciоromeite (with Ca). Since the copper content is significant in this phase, the green-olive tint prevails. Broadly speaking, all minerals in CHM 9 and CHM 10 could be weathering products of lead-bearing sulfidic ores deposit including fahlore-type minerals. The same may apply for CHM 12, given that the sample was discovered together with CHM 9 and CHM 10, and bears microscopic and macroscopic resemblance.

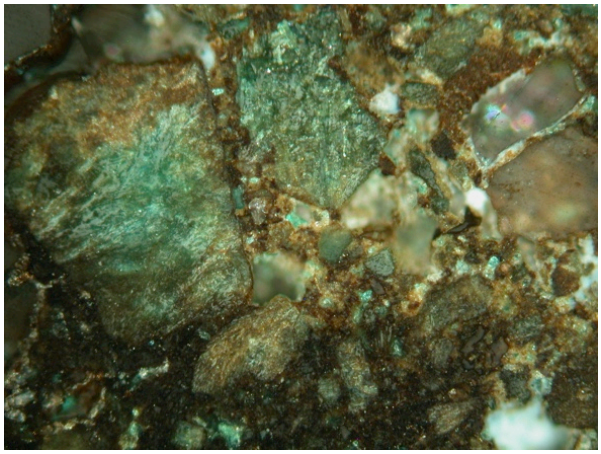

Figure 10: Photomicrograph of CHM 12 (location 3) under cross polarised light (magnification 100x, width 1 mm). Similarly to sample CHM 9 (Fig. 10), this sample is mixed with soil and iron oxides (orange/red).

The copper minerals with high sulfur content are CHM 1 and 5 (Figure 11). Compositionally, they represent a mixture of copper oxides/carbonates and sulfides, with high readings of arsenic, antimony, zinc and iron between them (Tables 5 and 6). The copper oxide/carbonate phases are optically dark and light grey, with the latter compositionally resembling olivenite (Cu:As is roughly 2:1), with some zinc (Table 5). Olivenite [$Cu_2(AsO_4)(OH)$] is a relatively common secondary copper mineral usually found in the oxidized zones of copper deposits containing arsenic-bearing phases, particularly tennantite, enargite, and others. The colour of this mineral varies from olive green to yellow and dark green (Dana and Ford, 1922: 603). A similar colour is also found in zinc-bearing olivenite [$CuZn(AsO_4)(OH)$].

The composition of sulfidic phases in both CHM 1 and 5 (Table 6) is closest to stibioenargite [$Cu_3(Sb,As)S_4$], or antimony-bearing enargite, which is chemically close to the tennantite and tetrahedrite (=fahlore) series, altogether classified as sulfosalts, generally similar to the phases observed in CHM 9 and 10. The colour of these minerals is usually steel grey, or dark, as observed in the cross-sections of samples in Fig. 3. Overall, and despite the general compositional differences, minerals CHM 1, 5, 9 and 10 (and possibly 12) could have originated from a similar deposit of lead and zinc-bearing fahlores, with oxidic minerals collected from near-surface weathering zones. Their aesthetic appeal could have been the decisive factor in the initial selection, particularly

given that the green component was predominant (copper), mixed with metallic-grey enargite. The latter could have also resembled galena, which was also used at Çatalhöyük.

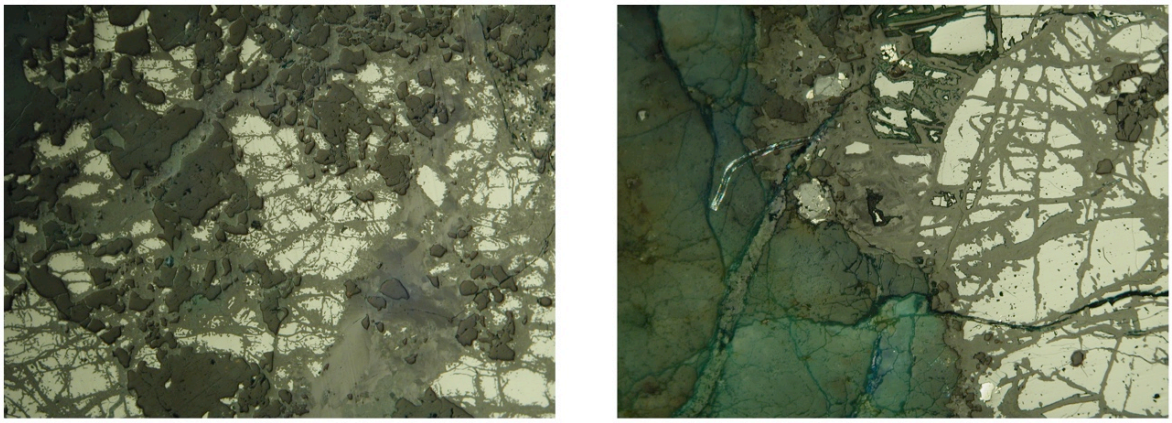

Figure 11: left) Photomicrograph of CHM 1 under cross polarised light (magnification 50x, width 3.2mm); right) Photomicrograph of CHM 5 under cross polarised light (magnification 50x, width 3.2mm). The white/bright phases have significant levels of Sb, As, Pb and Cu. The pale/white phases in both samples are sulfide-rich one, most likely Sb-bearing enargite. The grey and light grey phases are copper oxides with varying levels of As, Sb and Zn.

3.2. Metallurgical 'slag'

Neuninger et al. (1964) had identified one 'slag' sample in the analysed assemblage, CHM 11. Although this sample consists of 15 small items (each given a location number, see Fig. 5), they probably originate from the same crumbly lump, given that their structural characteristics are very similar. Interestingly, Neuninger et al. (1964) do not mention more than one 'slag' sample. The first impression from microstructural examination is that there is very little corrosion visible. Some locations, like No. 5 (Fig. 12f) contain copper corrosion products in their core, while there is little to none preserved on the outer edges on any other (for example see Figures 12j or 12l).

The most common feature in all locations are pale pink particles of metallic copper, which were, judging by their distinctive morphology formed *in situ* (Figures 12b, 12c, 12f, 12g, 13c), and never fully liquid. The reduction of copper ore to copper metal can happen at the solid state at temperatures from c. 700 °C upwards (Pollard et al., 1991), while the melting of copper metal requires temperatures in excess of 1083 °C. Hence, the clusters of metallic particles in our case are most likely a testimony of a solid-state process of reduction of copper oxide into copper metal, or one that happened at the threshold of conditions required to produce fully liquid copper metal.

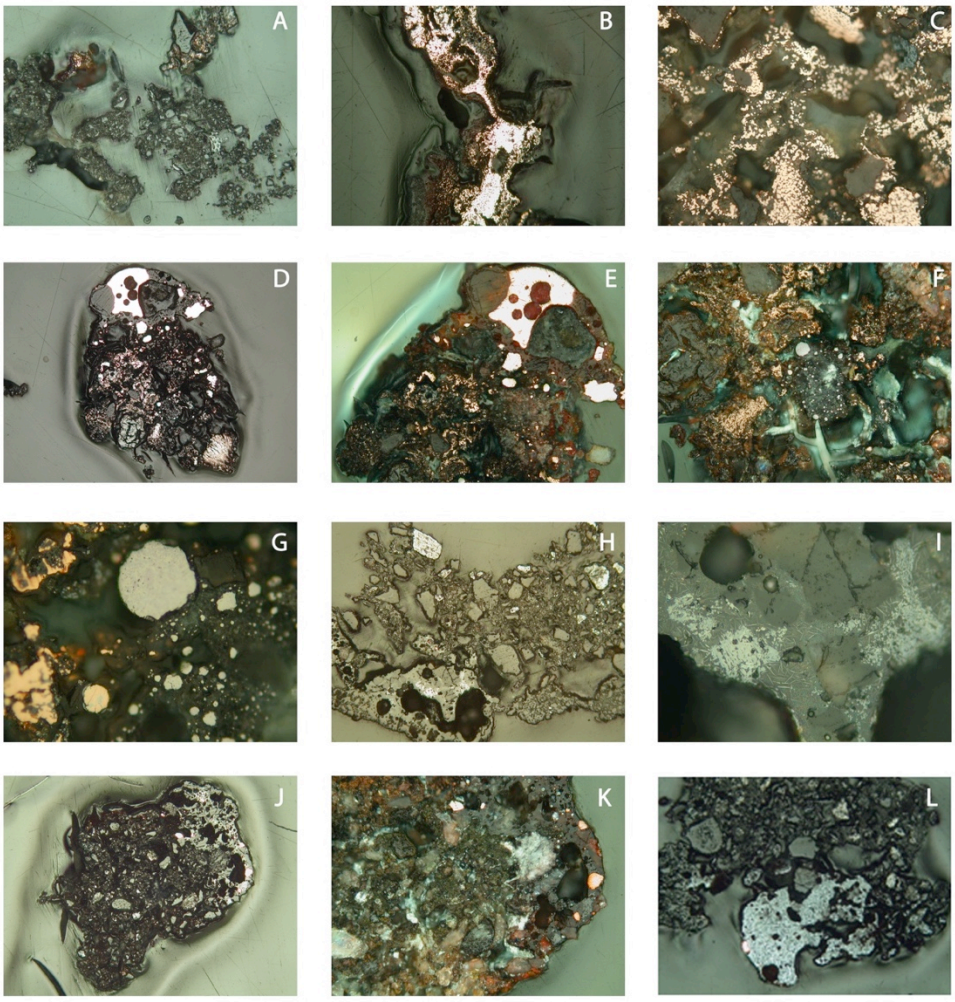

Figure 12: Photomicrographs of various locations in sample CHM 11 taken under both plain (ppl) and cross polarised (xpl) light.a) Photomicrograph of location 4 (magnification 100x, width 1mm, ppl). Note 'cold' core of the sample and metallic copper on its periphery, with cellular structure of a remaining charcoal (light grey); b) Photomicrograph of location 7 (magnification 100x, width 1mm, ppl). Note globules of metallic copper formed in situ, surrounded by copper oxides; c) Photomicrograph of location 2 (magnification 500x, width 0.34mm, ppl). Note globules of metallic copper formed in situ; d) Photomicrograph of location 5 (magnification 50x, width 3.2mm, ppl). Note metallic copper suspended in a slag matrix (top) and a mix of quartz and metallic copper formed in situ in centre and bottom; e) Photomicrograph of location 5 (magnification 50x, width 2mm, xpl). Note metallic copper and slag matrix (top) and 'cold' centre with metallic copper globules and corroded copper (oxide/carbonate); f) Photomicrograph of location 5 (magnification 100x, width 1mm, xpl). Note white metallic globules in a grey matrix (centre) surrounded by globules of bright copper metal and copper oxides (green and red phases); g) Photomicrograph of location 5 (magnification 500x, width 0.2mm, ppl). Note bright metallic globules with light grey and grey eutectic phases surrounded by copper metallic globules; h) Photomicrograph of location 8 (magnification 100x, width 1mm, ppl). Note 'cold' core and top of the sample, and slag matrix at the bottom left periphery; i) Photomicrograph of location 8 (magnification 500x, width 0.2mm, ppl). Note under higher magnification lathes of delafossite and spinel agglomerations embedded in slag matrix; j) Photomicrograph of location 11 (magnification 50x, width 2mm, ppl). Note 'cold' core and top right corner of the sample with slag matrix and metal prills embedded in it; k) Photomicrograph of location 11 (magnification 100x, width 1mm, xpl). Note heterogeneous 'cold' core with green patches of corroded copper, and 'hot' periphery with slag, copper metal and copper oxides; l) Photomicrograph of location 13 (magnification 50x, width 2mm, ppl). Note 'cold' core and 'hot' periphery at the bottom with cuprite and a metal prill.

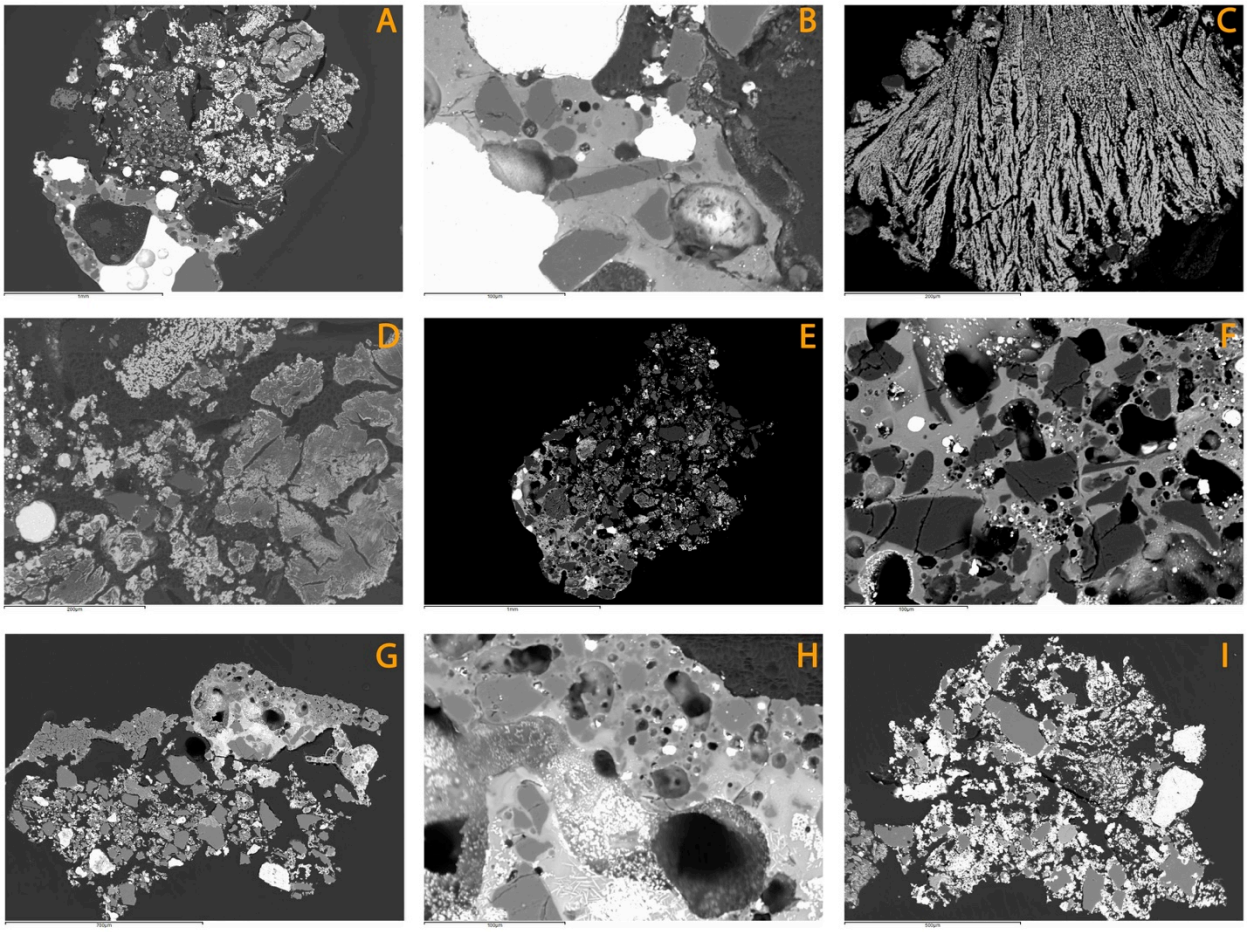

Figure 13: Backscattered electron images of four different locations (left to right): 5, 11, 8 and 9 in sample CHM 11. a) Location 5 (magnification 45x, width 2.5mm). Note slag matrix (light grey) with partially reacted (dark grey) and metallic phase (bright) in the bottom part, and a mix of metallic globules (dross) and quartz in the middle; b) Location 5 (magnification 400x, width 250 µm). Note bright copper metal phases and partially reacted quartz (dark grey) embedded in slag matrix; c) Location 5 (magnification 250x, width 450 µm). Note bright copper metallic globules forming within the mineral-like structure of copper oxide present in this sample; d) Location 5 (magnification 200x, width 450 µm). Note a mixture of convoluted agglomerations of copper oxide mixed with bright globules of copper metal and a light grey metal prill in the left bottom corner (antimonial copper); e) Location 11 (magnification 50x, width 2.5 mm). Note slag matrix (light grey) with copper metal prills (bright) and partially reacted quartz (dark grey) in left bottom and core with a few bright globules of copper metal in the middle; f) Location 11 (magnification 350x, width 250 µm). Note partially reacted quartz grains in a bright metal-speckled slag matrix; g) Location 8 (magnification 80x, width 1.4mm). Note slag matrix (light grey) with partially reacted quartz and bright phases suspended in it; h) Location 8 (magnification 400x, width 250 µm). Note bright spinel agglomerations and lathes of delafossite surrounded by partially reacted quartz and embedded in slag matrix. i) Location 9 (magnification 100x, width 1.2 mm). Note bright globules of copper metal throughout the item, with partially reacted and unreacted quartz.

Nevertheless, there are two locations in CHM 11 (location 5 and 11) where the copper metal appears as fully chemically and physically transformed (Figures 12d, 12e, 12j, 13a, 13b), forming pools of liquid metal in a glassy slag matrix speckled with dark red patches of copper oxide. In location 8 (Figures 12h, 12i, 13h), the slag matrix formed two distinctive phases: straight lathes of delafossite and convoluted agglomerations of iron-rich oxides (see below for analyses).

Significantly, the position of the molten phases/slag in the observed items is predominantly at their edges, not their cores (Figures 12d, 12e, 13a). The cores are, almost by rule, populated with specks and agglomerates of metallic copper (not molten throughout), quartz grains and an unreacted copper-oxide rich matrix (e.g. Figures 12c, 13g, 13g, 13i). Neuninger et al. (1964: 100) also noticed this and characterised the studied item (probably only loc. 5 here) as a 'combination of a porous molten material with natural mineral structure'. Such position and morphology of these fully liquefied phases in locations 5, 8 and 11 is telling of a high-temperature impact and reducing conditions that took place on the outer surface of some fragments in CHM 11, but failed to reach throughout the material. Given that these patches of fully liquefied phases represent 'true' slag, we will give a more detailed analytical account of these areas below. The mostly unreacted ('cold') core in the majority of observed items is the evidence of this thermal impact not reaching sufficiently high temperatures long enough to transform them into a fully liquefied (slag and metal) mass, like the one observed on the edges of three out of fifteen locations in sample CHM 11.

Bulk composition of the slag matrix

The slag in locations 5, 8 and 11 is heterogeneous, containing metal prills and partially reacted quartz in locations 5 and 11, and delafossite instead of metal prills in location 8, all present to different extents and embedded in a matrix of crystallised slag glass (Figures 12, 13). All locations are dominated by a significant copper (oxide) content. The bulk chemical analyses of the 'true' slag portions of these locations were conducted in areas relatively free from corrosion with the main aim of understanding their formation.

The bulk composition of slag in locations 5, 8 and 11, including all primary phases, shows that major oxides (silica, alumina, iron and copper oxides) add up to c. 77wt% on average. Lime, potash, magnesia and phosphorus oxide contribute c. 19wt% mean sum, and ore contamination (zinc and lead oxides) amounting up to c. 7.3wt% in location 5 (Table 7). Significant differences in the bulk slag composition, particularly in location 5, affect lime (c. 23wt% mean), which is four to five times higher than in the other two locations. This might be an indication of either a higher fuel ash content, or lime coming from both ore and fuel contamination (see example in Radivojević and Rehren, 2016: 224, Fig. 11). The contamination from ore elements (zinc and lead oxides) is only present in this location, and is reflected also in the composition of the glassy slag matrix (Table 8).

Spot analyses of the glassy slag matrix were conducted in areas relatively free of copper-rich phases or residual quartz. The major oxide distribution is similar to the bulk analyses, despite the lower copper content (Table 8).

The ore contamination is the most significant in location 5 (zinc and lead oxides at 7.5 wt%). The silica to alumina ratio is 4:1 in both locations 8 and 11, while in location 5 it is around 15:1. This observation identifies locations 8 and 11 as those containing a metallurgical slag, while location 5 appears more affected by silica-rich fuel ash.

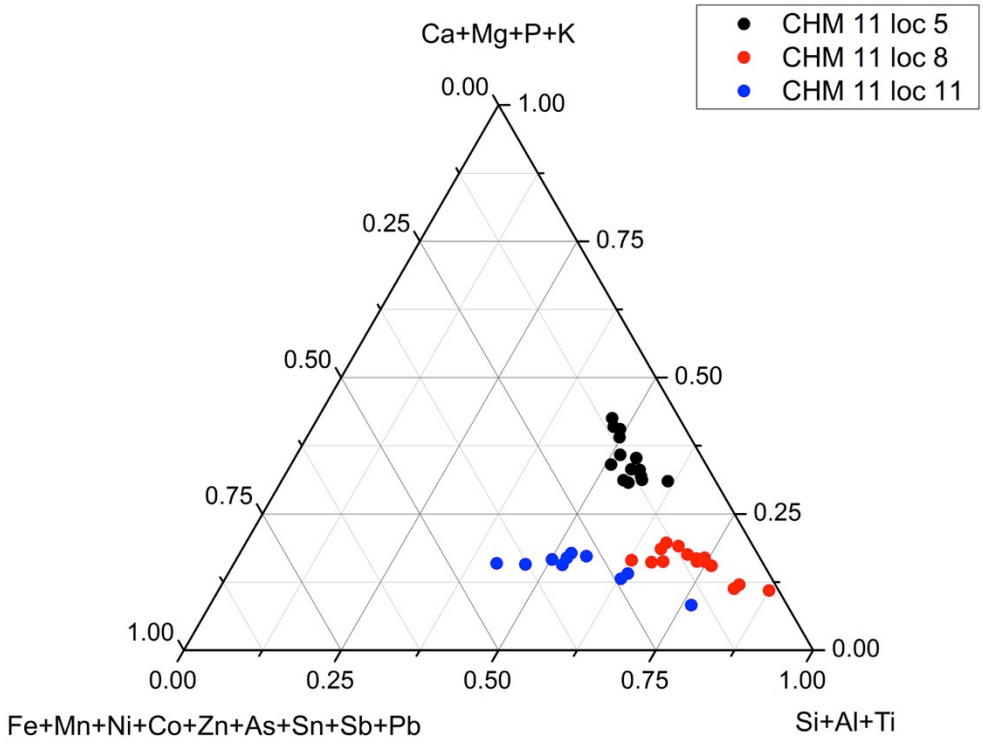

Figure 14: The ternary plot of compositional values of Si/Al/Ti-Ca/Mg/P/K-Fe/Zn/As/Sb/Pb oxides in glassy slag matrices in CHM 11, locations 5, 8 and 11. All values re-cast as Cu-free oxides.

The ternary plot (Fig. 14), representing all components influencing the formation of slag: ceramic/soil (SiO_2/Al_2O_3/TiO_2), fuel ash (CaO/MgO/P_2O_5/K_2O) and ore (FeO/ZnO/As_2O_3/Sb_2O_3/PbO), illustrates well the differences in the studied locations in sample CHM 11. The locations produce slightly distinctive patterns by their predominant formation by acidic oxides (SiO_2/Al_2O_3/TiO_2 corner, location 8), stronger intake of fuel component (location 5), or ore contamination (location 11), respectively.

Copper oxides are the dominant phase in all locations in CHM 11, as newly generated phases or as corrosion products. It is mostly found as a copper 'dross' outside the slag matrix, with traces of Zn and As. Tenorite was found in locations 3, 12 and 13 (Fig. 5), with only one measurement showing Zn (5 at%, location 13) in addition to copper. These metal oxide-rich 'dross' areas, are indicative of copper melting events (Bachmann, 1982), although they also occur in very early examples of copper smelting, like in the Balkans (Radivojević et al., 2010; Radivojević and Rehren, 2016) or in Iberia (Müller et al., 2004).

Delafossite, $Cu^{1+}Fe^{3+}O_2$, is usually recognised optically as straight lathes embedded in the glassy matrix (Table 9, Figures 12i, 13h) and mixed with iron spinels in convoluted agglomerations embedded in the slag matrix. Its co-occurrence with cuprite in a sample indicates fairly oxidising conditions of the melt, bordering the partial oxygen pressure required to reduce copper from cuprite (Müller et al., 2004: 40). It forms both during melting and smelting (see Bachmann, 1982: 16 for melting; and Hauptmann et al., 1993: 566; Hauptmann, 2000: 147 for smelting examples).

Iron spinels form characteristic grey cubic crystals in the glassy matrix, corresponding to the general formula $A^{2+}B_2^{3+}O_4^{2-}$. In both locations 11 and 15, they are found intergrown with delafossite in convoluted agglomerations, containing copper in addition to predominant iron (Table 9), as well as impurities coming from the surrounding slag matrix.

Metal prills and particles are found both suspended in the slag matrix and freely forming in other 'cold' areas throughout different locations (see Figures 12, 13). SEM-EDS analyses revealed almost pure copper with occasional presence of Sb and S (at c. 1 at%). LA-ICP-MS analyses (Table 10, Fig. 15) of the copper metal prills embedded in the peripheral slag matrix of location 5 showed the copper to contain As, Sb and Ni, consistent with the copper composition being reduced from malachite with some admixture of mostly antimonial fahlore.

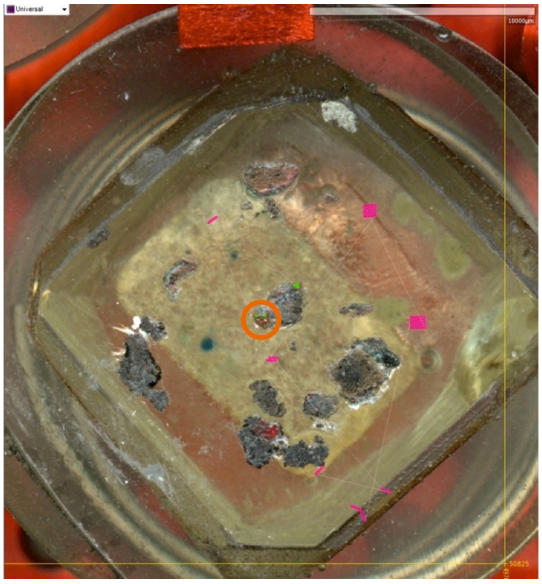

Figure 15: The orange circle indicates the location of copper metal phase analysed by LA-ICP-MS in sample CHM 11 (loc. 5) from Çatalhöyük.

Location 5 also includes optically pale metal prills that contain a eutectic of a light grey and a grey phase (Figures 12f, 12g, 13d). SEM-EDS analyses showed that they are antimonial copper (Table 11), with c. 25 at% of Sb in both phases, and a significant intake of Pb in the latter (c. 15 at% on average). This clearly reflects the original mineral, pointing at the tetrahedrite mineral series, similar to the phases observed in CHM 1, 5, 9 and 10

(Tables 4-6). These pale metal prills formed outside the slag matrix, in the cold 'core' of the location 5, and are surrounded by metallic particles of copper, interpreted above as very likely produced *in situ*. It is therefore equally likely that the antimonial copper prills were created in the same way, under conditions long and hot enough to ensure the *in situ* metal reduction but not the thorough melting of slag and copper in this location. Antimonial copper of this composition melts at around 650 °C, a temperature obviously exceeded in this spot as indicated by the prills' shape. The occurrence of such a compositionally distinctive phase only in location 5 in sample CHM 11 matches the compositional variability of the mineral fragments presented above, and further corroborates the assumption of it representing an incomplete *in situ* smelting event, not reaching conditions sufficient to homogenise the molten metal beyond a fraction of a millimetre. Effectively, location 5 mirrors the diverse composition of a mineral association that included pure copper minerals as well as antimonial fahlore, similar to that already seen in the copper minerals from the same archaeological context of grave 5, building E.VI.1 (CHM 9, 10 and 12) and other contemporary buildings in Level VI.

3.4. Metal beads

We re-cast the existing blocks of the metal beads CHM 14, 15, 30, 34 and 35. These represent individual metal artefacts, barring CHM 15, which consists of four locations (2-5) (Fig. 6). CHM 13 and 16 (a metal bead from each assemblage) were analysed for their lead isotope ratios only.

All beads were heavily corroded with little if any metal left. The surviving structure showed that they were worked into their shape by hammering, as seen in the orientation of (corroded) grains, e.g. in CHM 14, 15 (loc. 3), 30, 34 and 35 (Figures 16a, 16d, 16g, 16h and 16i). Metal bead CHM 34 in particular preserved the elongated direction of grains in the corroded metallic structure, thus indicating the heavy hammering work conducted on it (Fig. 16h). A metal bead in CHM 15 (location 2, Figures 16b, 16c) has annealing twins in the preserved copper metal, indicating that the last working step for this artefact was heating above the recrystallization temperature for copper to soften the metal. Thus, the beads were made in a sequence of steps already recognised for copper beads from this site (Neuninger et al., 1964; Birch et al., 2013), and in Anatolia in general, from as early as the 8th mill cal BC (e.g. Stech, 1990; Yalçın and Pernicka, 1999; Özdoğan and Özdoğan, 1999; Maddin et al., 1999). To produce these beads, native copper was hammered into sheet, divided into strips, rolled and cut, and subsequently worked and annealed. Although we were able to positively recognise this only in sample CHM 15 (loc. 2), we are confident in the light of the regional and contemporary evidence that this working procedure was applied to all copper artefacts from the site of Çatalhöyük, too.

LA-ICP-MS analysis of the metal phases in CHM 15 (locations 2 and 3) revealed pure copper metal, with very low concentrations of trace elements (Table 10, Fig. 17). From the pattern of the trace elements with silver and arsenic as the only elements that could be quantified (except for silicon, certainly part of the host rock), it can safely be concluded that this bead was made of native copper.

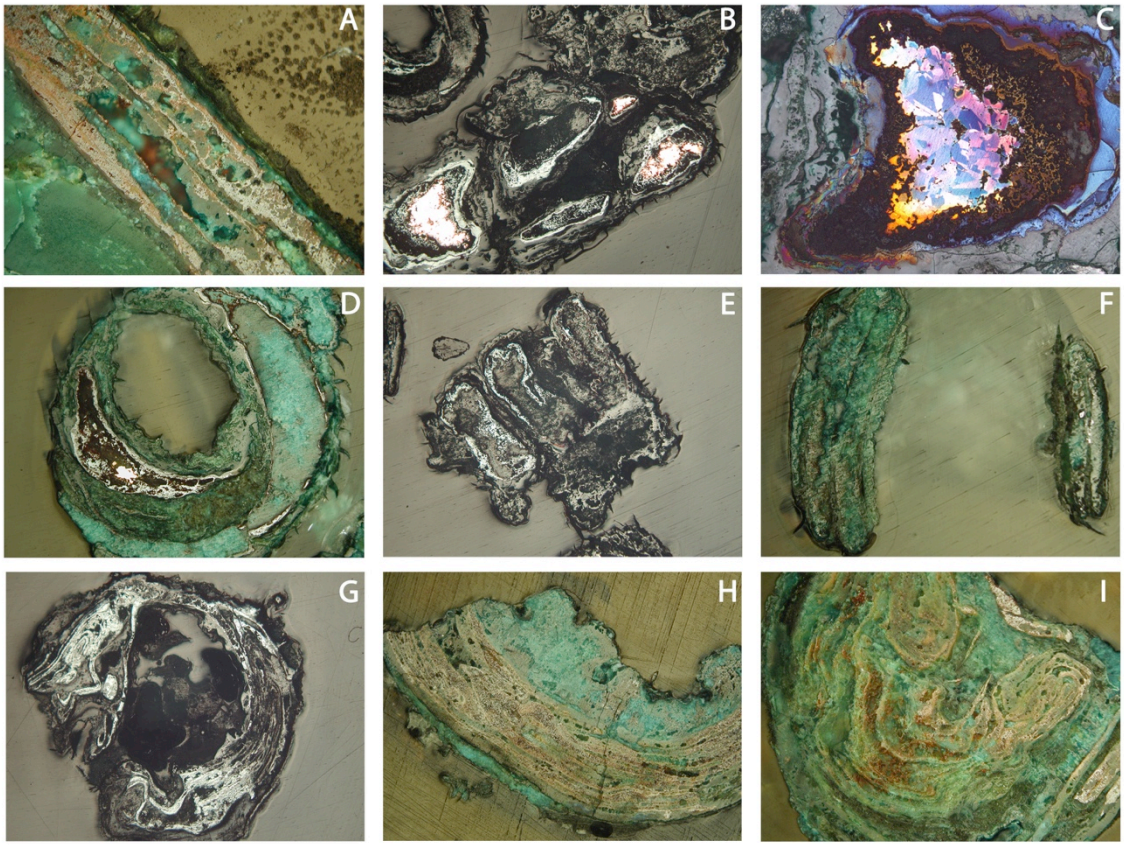

Figure 16: Photomicrographs of metal beads from Çatalhöyük taken under both plain (ppl) and cross polarised light (xpl). a) Photomicrograph of CHM 14 (magnification 100x, width 1mm, xpl). Note green corrosion inside a porous copper metal sheet; b) Photomicrograph of CHM 15, location 2 (magnification 25x, width 6.4mm, ppl). Note still preserved shiny copper metal amongst corrosion layers that outline a minimum of four structures/objects welded together due to post-depositional processes; c) Photomicrograph of CHM 15, location 2 (magnification 200x, width 0.6 mm, ppl). Note the 'natural' etching effect coming out of an extensive polishing. The grain structure shows evidence of working/hammering and annealing; d) Photomicrograph of CHM 15, location 3 (magnification 50x, width 3.2mm, xpl). Note the shiny copper metal and the outlines of corrosion products revealing the circular shape of a metallic bead; e) Photomicrograph of CHM 15, location 4 (magnification 25x, width 6.4mm, ppl). Note at least three structures/objects that corroded together; f) Photomicrograph of CHM 15, location 5 (magnification 50x, width 3.2mm, xpl). Note the outline of a circular bead with several preserved spots of copper metal amongst corrosion products; g) Photomicrograph of CHM 30 (magnification 25x, width 6.4mm, ppl). Note the circular shape of a bead made out of corrosion only; h) Photomicrograph of CHM 34 (magnification 50x, width 3.2mm, xpl), Note a shape of a fragmented metal bead outlined with a corrosion product. The metallic part (in the middle) retained still visible shape of elongated grains in its structure, a result of an intensive hammering work conducted in order to gain a desired shape of this object; i) Photomicrograph of CHM 35 (magnification 50x, width 3.2mm, xpl). Note a thick-walled metallic bead with corrosion layers growing out of folding lines (see top right for this detail).

Metal beads CHM 13 and CHM 15 were studied for provenance with lead isotope analyses (Table 12). A comparison of the lead isotope ratios of the two samples with the available data of copper ores in Turkey (Seeliger et al., 1985; Wagner et al., 1986; Wagner et al., 1989; Yener et al., 1991; Begemann et al., 2003, and

unpublished data from Curt-Engelhorn-Zentrum Archäometrie, Mannheim) finds the closest parallels in northeastern Turkey at Murgul and Gümüshane in the Artvin province (Fig. 18). There is also one sample from Ikiztepe near Kirklareli in Turkish Thrace (Fig. 19) that seems to match but this is a rather unlikely provenance. However, when taking into account ^{204}Pb in the denominator (Fig. 20), it is clear that no complete match is to be found in the available data. In this diagram the closest sample is from Esendegirmentepe in the Nigde province (Yener et al., 1991), which would also be geographically closest to Çatalhöyük, however, since other lead isotope ratios of these beads do not show consistency with this location, we must exclude it as a possible source. In summary, the geological origin of the studied samples remains unknown at this point.

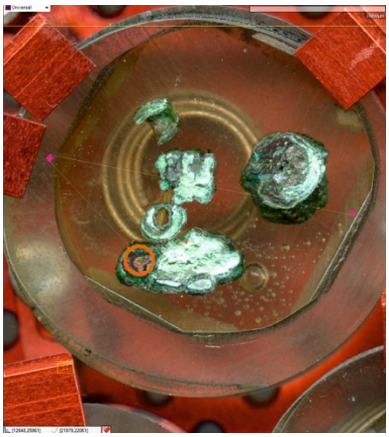

Figure 17: The orange circle indicates the location of copper metal phase analysed by LA-ICP-MS in sample CHM 15 from Çatalhöyük.

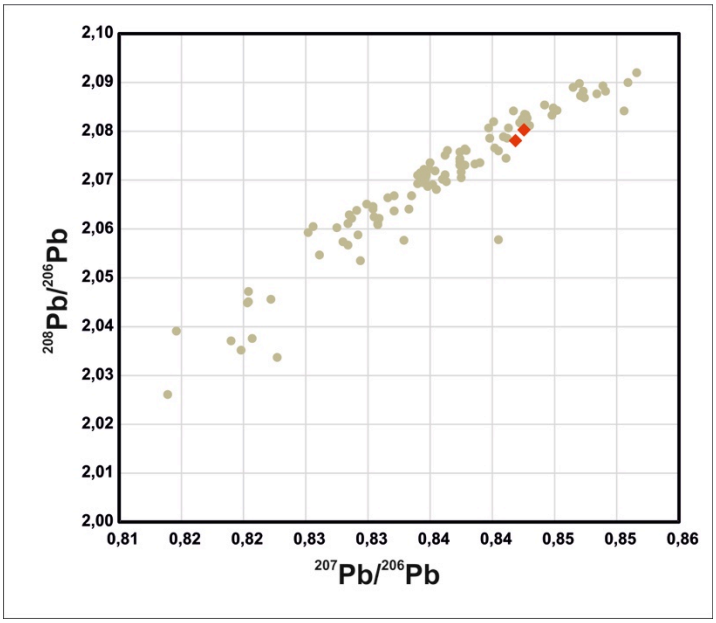

Figure 18: Overview lead isotope ratios of copper ore samples from Turkey compared with samples CHM 13 and CHM 16 from Çatalhöyük in red.

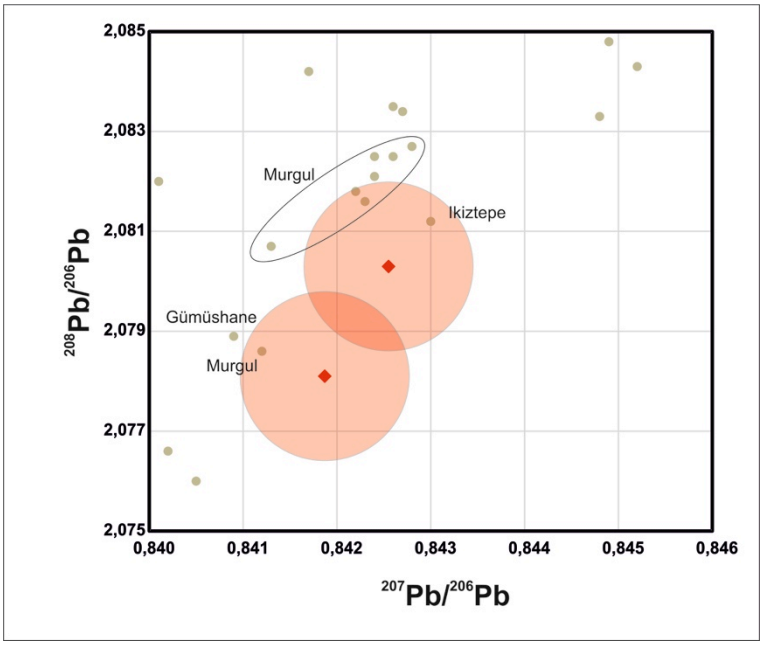

Figure 19: Detailed comparison of Turkish copper ores with the two samples CHM 13 and CHM 16 from Çatalhöyük in red. The red halos comprise data within 0.1% of the copper samples. No consistency has been found with the available dataset.

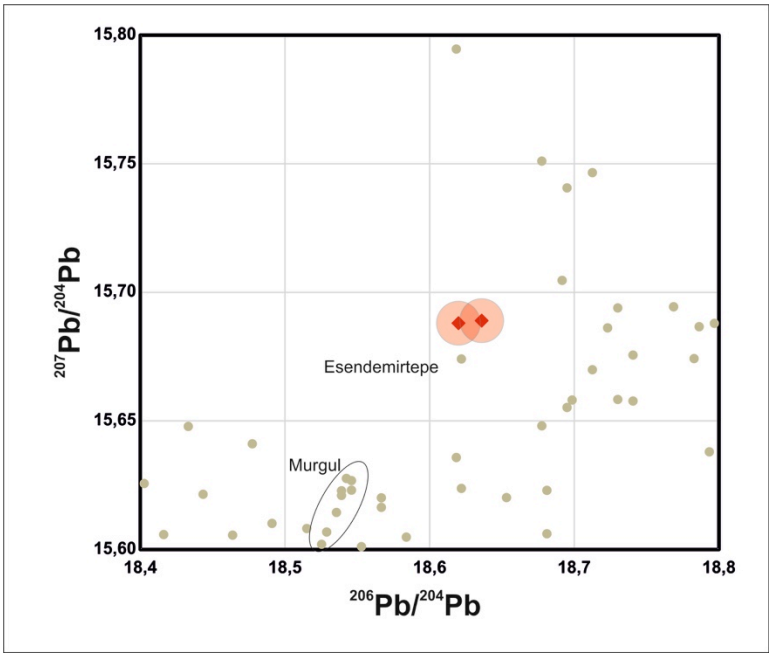

Figure 20: Alternative diagram for the detailed comparison of Turkish copper ore with the two samples CHM 13 and CHM 16 from Çatalhöyük (in red). The red halos comprise data within 0.1% of the copper samples. No consistency has been found with the available dataset.

4. Discussion

The analyses above identify two distinctive groups of materials in the studied assemblage from Çatalhöyük: copper minerals and the 'slag' samples form one related category of materials, while copper metal beads make another.

The underlying criterion that links the copper minerals with a 'slag' in the same group is the distinctive chemical signature dominated by copper, and also containing zinc, lead, antimony and arsenic. These elements were found in mineral-based samples CHM 1, 5, 9, and 10 (in various ratios), as well as in the glassy slag matrix and some metal prills in CHM 11. Although different minerals were identified in the samples, it is important to emphasise their close geological relationship in nature. Broadly speaking, they probably originate from a weathered hydrothermal copper deposit with lead and zinc-bearing sulfidic minerals including the tennantite and tetrahedrite series, like (antimony-bearing) enargite and other fahlore-type minerals. Specimens from such a deposit would also be aesthetically appealing, with a colour palette dominated by different shades of green (for instance from malachite), including shades from pale/yellow to metallic grey or black. Noteworthy in this context is the crumbly nature of studied minerals, which macroscopically finds parallel with the hand-crushed pigments deposited in a few Çatalhöyük burials (see Fig. 2).

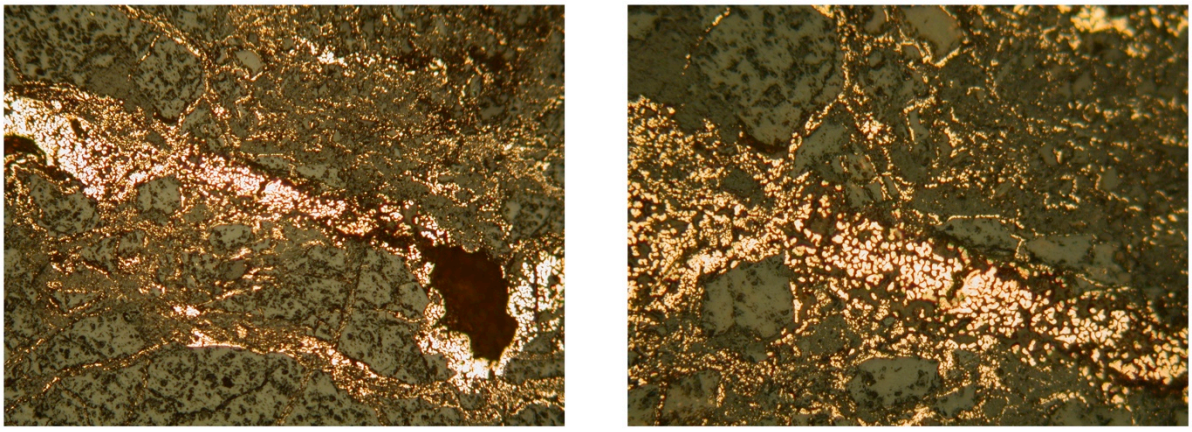

Figure 21: Photomicrographs of experimentally produced metallic globules 'in situ', in an hour long experiment in Serbia in 2013, taken under the plain polarised light (left: magnification 100x, width 1mm; right: magnification 200x, width 0.5mm). Note similarity with Figures 12c or 12f.

4.1. CHM 11: Metallurgical slag?

This combination of elements closely links the mineral samples to the only 'slag' sample in the studied collection, CHM 11. It consists of finely scattered copper particles with discrete prills of a metal phase rich in

antimonial copper in location 5 (Table 11, Figures 12f, 12g). Its morphology and immediate surrounding appear as formed 'in situ' in an environment that did not reach full liquefaction, thus preventing a merging of the individual metal particles to a few larger prills. As an illustration to the 'in situ' solid state production of metallic copper, preserving the original outline of the copper mineral despite its reduction to copper metal, we show in Fig. 21 results from a copper smelting experiment conducted by the first author in Serbia in 2013. The slag produced after a short-lived thermal impact shows an incompletely liquefied area populated by small copper particles that transformed chemically from the initial copper oxide, but failed to amalgamate into larger prills. The principle of such solid-state metal reduction without producing a molten metal phase is well known from bloomery iron smelting, which produces very similar structures.

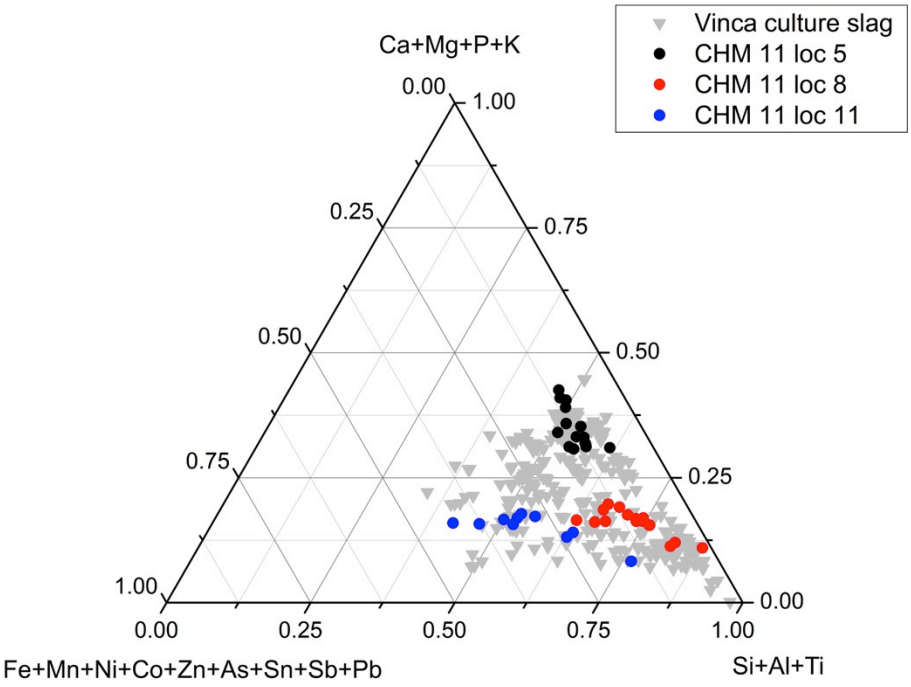

Figure 22: The ternary plot of compositional values of Si/Al/Ti-Ca/Mg/P/K-Fe/Zn/As/Sb/Pb oxides in glassy slag matrices in CHM 11, locations 5, 8 and 11, plotted against values from the Vinča culture slags from the sites of Belovode, Vinča and Gornja Tuzla in Serbia and Bosnia and Herzegovina (data from Radivojević et al. 2010; Radivojević 2012; Radivojević 2015; Radivojević and Rehren 2016). All values re-cast as Cu-free oxides.

Metallic particles of copper that possibly formed below melting temperature (cf. Pollard et al., 1991) are common throughout all locations in CHM 11, more often embedded in baked soils rather than proper slag. Islands of glassy slag matrix formed at the outskirts of only three out of fifteen locations within CHM 11, consisting of a 'true' slag phase with fully molten (antimonial) copper prills and newly-formed crystals of cuprite, delafossite and iron spinels. Their paragenesis in a slag matrix illustrates variable, and slightly reducing conditions, sufficient to smelt copper (cf. Elliott, 1976). However, despite the formal conditions for smelting being met, it is difficult to identify intentionality in this pattern. Another indicator of a haphazard nature of

exposure of different locations in CHM 11 to high temperatures is the slags' diverse compositional patterns (Fig. 14). The three locations with slag matrix in their outskirts differ considerably in their intake of the three major components in slag formation: minerals, fuel ash, and ceramic/soil.

The compositional values extracted from these 'islands' of glassy slag matrices are corresponding well to the values obtained from c. 7000 years old metallurgical slag samples from three different Vinča culture sites in Serbia (Fig. 22), with which they also share common phase associations and textures (Radivojević et al., 2010; Radivojević, 2012; Radivojević and Rehren, 2016: 215 ff., Fig. 6). In effect, this ternary plot confirms that the glassy slag areas from CHM 11 are indeed similar to the earliest known metal smelting evidence to date.

However, the context of the observed glassy matrices in Çatalhöyük's CHM 11 and Vinča slag samples highlights important differences: while the Vinča slags, despite being highly viscous and heterogeneous, are liquefied throughout (Radivojević and Rehren, 2016), the slag in CHM 11 is a peripheral formation to a core that has not been exposed to the ash of some organic material near-by which acted as a flux to produce a liquid slag on the surface of some fragments. The haphazard nature of the slag phase formation in CHM 11 underlines the accidental nature of these three out of fifteen locations in the mentioned sample (Fig. 5). Their overall heterogeneous nature is a result of a compositional rather than a thermal gradient, even though the vitrification is predominantly on the surface of the fragments as if they were affected by a short direct exposure to fire. Compositional heterogeneity is a normal feature of a fine-grained rock or a powder with a mixture of minerals which on its surface was fluxed by ash, while the temperature would have been the same across such a small sample with minute size inclusions as in sample CHM 11 which was slowly baked as part of a burial affected by a major conflagration above it.

In addition, the solid-state formation of metallic copper particles alongside similarly shaped antimonial copper in location 5 in CHM 11 illustrates the reduction of a mineral association that contained both pure copper minerals and a fahlore-type mineral, as seen in the copper mineral fragments (CHM 9, 10 and 12) from the same context. Thus, any artefacts made from metal smelted from such a mixed ore would inevitably contain noticeable concentrations of elements such as antimony or lead naturally present in the green-grey minerals, but none of these have been found in any of the analysed copper metal artefacts from Çatalhöyük. Instead, their composition, as determined by LA-ICPMS, matches that of native copper (see also Birch et al. 2013), indicating that the demand for metallic copper was met by sources of the native metal, and not through smelting of copper ores.

We were unable to find evidence of an intentional smelting event at the site of Çatalhöyük directed towards extracting copper metal for further use. Therefore, we propose here that the 'slag' sample CHM 11 was produced accidentally, most likely when a collection of minerals was caught up in a fire event in building E.VI.1, earlier reported by Mellaart (1964: 85) as carbonizing skeletons and burial goods buried up to 3 feet (c. 90 cm) deep. Hence, the 'slag' sample (CHM 11) is best termed as a *partially vitrified mixture of minerals and soil*, which

happened to be the most heat-exposed specimen in the contextually associated collection of samples (CHM 9-12).

Considering the nature of their context and the miniature size of the studied 'locations', it appears very likely that these samples were originally deposited in the burial (*Grave 5 from the central platform*) as hand-crushed green or blue minerals, and then burned in a post-depositional fire. This matches the documented contexts of burial deposition of green (malachite) or blue (azurite) pigments that Mellaart reported (1964) as paint (on a skull) or as free lumps; similar finds originate from funerary contexts in the renewed excavations, too (Thornton, 2001). Çamurcuoğlu (2015) documented powdered malachite and azurite pigments coated with clay and iron oxide particles, which match closely what we see in Figures 2, 9 and 10, although our samples appear more finely dispersed in soil. Although green stones were used for artefact (bead) making in Çatalhöyük, it is important to emphasise that those stones were not malachite, but apatite, or similarly green-coloured minerals, in line with the argument that green colour was more important than the mineral type (e.g. Bar-Yosef Mayer and Porat, 2008). However, malachite was used at Çatalhöyük as a pigment in burial contexts, on which we base our interpretation for the nature of CHM 9 -12 samples studied here.

The copper metal beads analytically stand in stark contrast to all studied minerals, including the vitrified mineral CHM 11. The beads are all consistent with being made of native copper, clearly distinguishing them from the lightly antimonial copper seen in CHM 11. The composition and technology of working of these pure metal samples corresponds well with contemporary finds across Anatolia, while their provenance remains unknown.

5. Conclusions

For nearly half a century, Çatalhöyük has played a major role in the discussion of the inception of metallurgy, based primarily on the frequent reference Mellaart made to the occurrence of metal finds in layers as early as the 7th millennium cal BC, and the identification by Neuninger et al. (1964) of metallurgical slag in one of the samples they analysed. Careful reconciliation of the surviving documentation from Mellaart's excavations with the material record demonstrated beyond doubt that Mellaart used the word 'metal' in a very liberal sense, clearly including different minerals in that category. Unfortunately, the excavation records do not allow to pinpoint individual samples to specific contexts within individual houses to the level of detail one would expect today; however, Mellaart's enthusiasm to engage with scientific analysis at that time resulted in the survival and identification of this crucial and unique material. What remains particularly commendable is the great detail of excavation technique, which led to the recovery of miniature metallic samples from the soil, as exemplified in Fig. 5.

Detailed re-analysis of the CHM 9 -12 samples sent to Neuninger in the 1960s proved beyond doubt that only sample CHM 11 showed the formation of metallic copper from minerals, which prompted Neuninger et al. (1964) to define it as 'metallurgical slag'. Indeed, three out of 15 fragments within sample CHM 11 closely match the chemical and microstructural features known from very early smelting slag elsewhere (Bachmann, 1980; Müller et al., 2004; Höppner et al., 2005; Bourgarit, 2007; Radivojević et al., 2010; Radivojević, 2013), including the formation of small prills of antimonial copper and of a range of copper and iron oxides in a semi-molten and compositionally heterogeneous siliceous matrix. The remaining fragments are rich in finely dispersed copper particles apparently reduced in the solid state from some secondary copper minerals, whose outer shape they sometimes retain, without agglomerating into prills.

In the light of the analytical and contextual evidence, we interpret this material as the result of accidental copper reduction when some crushed green minerals in a burial context were baked in a post-depositional fire in dwelling E.VI.1 in Çatalhöyük, whose thermal effect reached not only these minerals/pigments, but also the bodies and burial items to a depth of at least 90 cm (see Mellaart, 1964; Angel, 1971; Burnham, 1965). These crushed green minerals might have been sprinkled over the body, or deposited in a pouch that decayed over time; the result of both processes would have been loose green mineral fragments (pigments?) scattered around the human remains. The accidental result of this event was the solid-state reduction of metallic (antimonial) copper and formation of peripheral copper slag in some of the surviving fragments. This process would have taken place in mildly reducing conditions created by the burning or charring of some organic matter in the burial; the ash of this would have led to the superficial vitrification ('slagging') of some of the mineral-rich particles.

Taken together, the evidence from Mellaart's 'metal' samples therefore is consistent with our understanding of the selection and different treatment of green minerals and native copper during the 7th millennium BC in Anatolia and surrounding regions, rooted in earlier practice and continuing for another couple millennia. A link from this material to the inception of metallurgy, however, has been finally put to rest, effectively removing from the discussion the already much-damaged this 'Exhibit #1' for a single origin of metallurgy. Conversely, this leaves intact the notion of probably independent origins of metallurgy in the Balkans and possibly Iran c. 1500 years later, at the turn of the 6th to the 5th millennium BC. It is beyond the remit of this paper to explore the socioeconomic and technical conditions leading to this broadly synchronous emergence of metallurgy in geographically widely separated regions. However, accepting multiple origins of metallurgy enables us to advance the focus of our research onto those parameters, which these progenitor cultures and metalliferous regions share, in order to identify the essential conditions leading to the invention and innovation of the controlled smelting of metal.

Authors' contributions

MR and ThR conceived, designed and coordinated the study and interpreted all data; SF and MR collected and interpreted contextual data; MR and EP carried out all analytical work and data processing; DC conducted pigments analysis; MR, ThR, SF and EP drafted the manuscript. All authors gave final approval for publication.

Acknowledgements

We owe a great debt of gratitude to Professor Gerhard Sperl for giving us full access to the material originally sent by Mellaart to Neuninger for analysis, and for providing all relevant documentation in his possession. This would not have been made possible without the generous support of Professor Ian Hodder. Much of the work was done while MR and SF were visiting researchers at UCL Qatar. Ana Franjić kindly re-polished the analysed material and Ljiljana Radivojević and Cordelia Hall prepared illustrations for publication. We are very grateful to Alex Bayliss for the interim statement, attached in the Supplementary Materials, on the chronology of Çatalhöyük. Qatar Foundation enabled the new study of this material through its generous funding of UCL Qatar as a joint centre of excellence for Museology, Conservation and Archaeology. Detailed comments from two reviewers helped us to better situate our research; any remaining shortcomings are ours.

Bibliography

Angel, J. L. 1971. Early Neolithic skeletons from Çatal Höyük: demography and pathology. *Anatolian Studies,* 21, pp. 77-98.

Bachmann, H.-G. 1982. *The Identification of Slags from Archaeological Sites,* London: Institute of Archaeology.

Bachmann, H. G. 1980. Early copper smelting techniques in Sinai and in the Negev as deduced from slag investigations. *In:* Craddock, P. T. (ed.) *Scientific Studies in Early Mining and Extractive Metallurgy.* London: British Museum, pp. 103-134.

Bar-Yosef Mayer, D. E. & Porat, N. 2008. Green stone beads at the dawn of agriculture. *Proceedings of the National Academy of Sciences,* 105, pp. 8548-8551.

Bayliss, A., Brock, F., Farid, S., Hodder, I., Southon, J. & Taylor, R. E. 2015. Getting to the Bottom of It All: A Bayesian Approach to Dating the Start of Çatalhöyük. *Journal of World Prehistory,* 28, pp. 1-26.

Begemann, F., Schmitt-Strecker, S. & Pernicka, E. 2003. On the composition and provenance of metal finds from Beşiktepe (Troia). *In:* Wagner, A., Pernicka, E. & Uerpmann, H.-P. (eds.) *Troia and the Troad: Scientific Approaches.* Berlin, Heidelberg: Springer-Verlag, pp. 173-201.

Bialor, P. A. 1962. The chipped stone industry of Çatal Höyük. *Anatolian Studies,* 12, pp. 67-110.

Birch, T., Rehren, Th. & Pernicka, E. 2013. The Metallic Finds from Çatalhöyük: A Review and Preliminary New Work. *In:* Hodder, I. (ed.) *Substantive Technologies at Çatalhöyük.* London, Los Angeles: British Institute at Ankara, Cotsen Institute of Archaeology, pp. 307-316.

Bourgarit, D. 2007. Chalcolithic copper smelting. *In:* La Niece, S., Hook, D. & Craddock, P. (eds.) *Metals and Mines: Studies in Archaeometallurgy.* London: Archetype Publications, pp. 3-14.

Burnham, H. 1965. Çatal Höyük - the textiles and twine fabrics. *Anatolian Studies,* 15, pp. 169-174.

Camurcuoğlu, D. S. 2015. *The Wall Paintings of Catalhoyuk (Turkey): Materials, Technologies and Artists. Unpublished PhD thesis.* University College London

Cessford, C. 2005. Absolute dating at Çatal Höyük. *In:* Hodder, I. (ed.) *Changing Materialities at Çatalhöyük: reports from the 1995-99 seasons.* Cambridge: McDonald Institute Monographs, British Institute at Ankara, pp. 65-100.

Cessford, C. & Near, J. 2005. Fire, burning and pyrotechnology at Çatalhöyük *In:* Hodder, I. (ed.) *Çatalhöyük perspectives: themes from the 1995-99 seasons.* Cambridge, London: McDonald Institute Monographs, British Institute of Archaeology at Ankara Monograph, pp. 171-182.

Craddock, P. T. 2001. From hearth to furnace: evidences for the earliest metal smelting technologies in the eastern Mediterranean. *Paléorient,* 26, pp. 151-156.

Dana, E. S. & Ford, W. E. 1922. *A Textbook of Mineralogy (with an extended treatise on crystallography and physical mineralogy),* New York: John Wiley and Sons.

Dougherty, R. C. & Caldwell, J. R. 1966. Evidence of Early Pyrometallurgy in the Kerman Range in Iran. *Science,* 153, pp. 984-985.

Elliott, J. F. 1976. Phase relationships in the pyrometallurgy of copper. *Metallurgical and Materials Transactions B. Process Metallurgy and Materials Processing Science,* 7, pp. 17-33.

Farid, S. 2007. Level VII. *In:* Hodder, I. (ed.) *Excavating Çatalhöyük: South, North and KOPAL Area reports from the 1995-99 seasons.* Cambridge, London: McDonald Institute Monographs, British Institute of Archaeology at Ankara Monograph, pp. 283-338.

Frame, L. D. 2012. Reconstructing ancient technologies: Chalcolithic crucible smelting at Tal-i Iblis, Iran. *In:* Jett, P., McCarthy, B. & Douglas, J. G. (eds.) *Scientific Research on Ancient Asian Metallurgy. Proceedings ofthe Fifth Forbes Symposium at the Freer Gallery of Art.* Washington, D. C.: Archetype Publications in association with the Freer Gallery of Art, Smithsonian Institution, pp. 183-204.

Glumac, P. & Tringham, R. E. 1990. The Exploitation of Copper Minerals. *In:* Tringham, R. E. & Krstić, D. (eds.) *Selevac, A Neolithic Village in Yugoslavia.* Los Angeles: University of California Press, pp. 549-563.

Golden, J. M. 2010. *Dawn of the Metal Age: Technology and Society during the Levantine Chalcolithic* London, Oakville, CT Equinox Pub.

Harrison, K., Martin, V. & Webster, B. 2013. Structural fires at Çatalhöyük *In:* Hodder, I. (ed.) *Substantive Technologies at Çatalhöyük: Reports from the 2000-2008 Seasons.* London, Los Angeles: British Institute of Archaeology at Ankara Monograph, Cotsen Institute of Archaeology Press, pp. 137-146.

Hauptmann, A. 2000. *Zur frühen Metallurgie des Kupfers in Fenan/Jordanien, Der Anschnitt, Beiheft 11,* Bochum: Deutsches Bergbau-Museum.

Hauptmann, A., Lutz, J., Pernicka, E. & Yalçin, Ü. 1993. Zur Technologie der frühesten Kupferverhüttung im östlichen Mittelmeerraum. *In:* Frangipane, M., Hauptmann, A., Liverani, M., Matthiae, P. & Mellink, M. (eds.) *Between the Rivers and over the Mountains: Archaeologica Anatolica et Mesopotamica Alba Palmieri Dedicata.* Roma: Dipartimento di Scienze Storiche Archeologiche e Antropologiche dell'Antichità, Università di Roma 'La Sapienza', pp. 541-563.

Helbaek, H. 1963. Textiles from Çatal Hüyük. *Archaeology,* 16, pp. 39-46.

Helwing, B. 2013. Early metallurgy in Iran - an innovative region as seen from the inside. *In:* Burmeister, S., Hansen, S., Kunst, M. & Muller-Scheessel, N. (eds.) *Metal Matters: Innovative Technologies and Social Change in Prehistory and Antiquity.* Rahden/Westf.: Verlag Marie Leidorf, pp. 105-135.

Höppner, B., Bartelheim, M., Huijsmans, M., Krauss, R., Martinek, K. P., Pernicka, E. & Schwab, R. 2005. Prehistoric copper production in the Inn Valley (Austria), and the earliest copper in central Europe. *Archaeometry,* 47, pp. 293-315.

Kavtaradze, G. L. 1999. The importance of metallurgical data for the formation of Central Transcaucasian chronology. *In:* Hauptmann, A., Pernicka, E., Rehren, Th. & Yalçın, Ü. (eds.) *The Beginnings of Metallurgy, Der Anschnitt, Beiheft 9.* Bochum: Deutsches Bergbau-Museum, pp. 67-102.

Kenoyer, J. M. & Miller, M.-L. 1999. Metal technologies of the Indus Valley tradition in Pakistan and western India. *In:* Pigott, V. C. (ed.) *The Archaeometallurgy of the Asian Old World.* Philadelphia (PA): University of Pennsylvania Museum, pp. 107-152.

Leusch, V., Pernicka, E. & Armbruster, B. 2014. Chalcolithic gold from Varna – Provenance, circulation, processing, and function. *In:* Meller, H., Risch, R. & Pernicka, E. (eds.) *Metals of Power-Early Gold and Silver. 6th Archaeological Conference of Central Germany, October 17-19, 2013, Halle.* Halle: Landesamt für Denkmalpflege und Archäologie Sachsen-Anhalt/Landesmuseum für Vorgeschichte, pp. 165-182.

Maddin, R., Muhly, J. D. & Stech, T. 1999. Early metalworking at Çayönü. *In:* Hauptmann, A., Pernicka, E., Rehren, Th. & Yalçın, Ü. (eds.) *The Beginnings of Metallurgy, Der Anschnitt, Beiheft 9.* Bochum: Deutsches Bergbau-Museum, pp. 37-44.

Maddin, R., Stech, T. & Muhly, J. D. 1991. Çayönü Tepesi. The Earliest Archaeological Metal Artefacts. *In:* Mohen, J.-P. & Éluère, C. (eds.) *Découverte du Métal* Paris: Picard, pp. 375-386.

Marciniak, A., Barański, M. Z., Bayliss, A., Czerniak, L., Goslar, T., Southon, J. & Taylor, R. E. 2015. Fragmenting Times: interpreting a Bayesian chronology for the late Neolithic occupation of Çatalhöyük East, Turkey. *Antiquity,* 89, pp. 154-176.

Mellaart, J. 1961. Early Cultures of the South Anatolian Plateau. *Anatolian Studies,* 11, pp. 159-184.

Mellaart, J. 1962. Excavations at Çatalhöyük: first preliminary report, 1961. *Anatolian Studies,* 12, pp. 41-65.

Mellaart, J. 1963. Excavations at Çatalhöyük, 1962: second preliminary report. *Anatolian Studies,* 13, pp. 43-103.

Mellaart, J. 1964. Excavations at Çatalhöyük, 1963: third preliminary report *Anatolian Studies,* 14, pp. 39-119.

Mellaart, J. 1966. Excavations at Çatal Höyük, 1965: fourth preliminary report. *Anatolian Studies,* 16, pp. 65-191.

Mellaart, J. 1967. *Çatalhöyük, A Neolithic Town in Anatolia,* London: Thames and Hudson.

Mickel, A. 2016. Tracing Teams, Texts, and Topics: Applying Social Network Analysis to Understand Archaeological Knowledge Production at Çatalhöyük. *Journal of Archaeological Method and Theory,* 23, pp. 1095-1126.

Muhly, J. D. 1989. Çayönü Tepeşi and the beginnings of metallurgy in the Old World. *In:* Hauptmann, A., Pernicka, E. & Wagner, G. A. (eds.) *Old World Archaeometallurgy, Der Anschnitt, Beiheft 7.* Bochum: Deutsches Bergbau-Museum, pp. 1-13.

Müller, R., Rehren, Th. & Rovira, S. 2004. Almizaraque and the early copper metallurgy of southeast Spain: new data. *Madrider Mitteilungen* 45, pp. 33-56.

Murillo-Barroso, M. & Montero-Ruíz, I. 2012. Copper ornaments in the Iberian Chalcolithic: technology versus social demand. *Journal of Mediterranean Archaeology,* 25, pp. 53-73.

Neuninger, H., Pittioni, R. & Siegl, W. 1964. Frühkeramikzeitliche Kupfergewinnung in Anatolien. *Archaeologia Austriaca,* 35, pp. 98-110.

Özdoğan, M. & Özdoğan, A. 1999. Archaeological evidence on the early metallurgy at Çayönü Tepeşi *In:* Hauptmann, A., Pernicka, E., Rehren, Th. & Yalçın, Ü. (eds.) *The Beginnings of Metallurgy, Der Anschnitt, Beiheft 9.* Bochum: Deutsches Bergbau-Museum, pp. 13-22.

Pernicka, E. 1990. Gewinnung und Verbreitung der Metalle in prähistorischer Zeit. *Jahrbuch des Römisch-Germanischen Zentralmuseums Mainz* 37, pp. 21-129.

Pernicka, E., Begemann, F. & Schmitt-Strecker, S. 1993. Eneolithic and Early Bronze Age copper artefacts from the Balkans and their relation to Serbian copper ores. *Prähistorische Zeitschrift* 68, pp. 1-54.

Pernicka, E., Begemann, F., Schmitt-Strecker, S., Todorova, H. & Kuleff, I. 1997. Prehistoric copper in Bulgaria. Its composition and provenance. *Eurasia Antiqua* 3, pp. 41-180.

Pigott, V. C. 1999. The development of metal production on the Iranian Plateau: an archaeometallurgical perspective. *In:* Pigott, V. C. (ed.) *The Archaeometallurgy of the Asian World.* Philadelphia (PA): University of Pennsylvania Museum, pp. 73-106.

Pollard, A. M., Thomas, R. G., Ware, D. P. & Williams, P. A. 1991. Experimental Smelting of Secondary Copper Minerals - Implications for Early Bronze-Age Metallurgy in Britain. *In:* Pernicka, E. & Wagner, G. A. (eds.) *Archaeometry '90: International Symposium in Archaeometry.* Basel: Birkhäuser, pp. 127-136.

Radivojević, M. 2007. *Evidence for early copper smelting in Belovode, a Vinča culture settlement in Eastern Serbia.* MSc Thesis, UCL Institute of Archaeology.

Radivojević, M. 2012. *On the Origins of Metallurgy in Europe: Metal Production in the Vinča Culture.* PhD Thesis, UCL Institute of Archaeology.

Radivojević, M. 2013. Archaeometallurgy of the Vinča culture: a case study of the site of Belovode in eastern Serbia. *Journal of Historical Metallurgy,* 47, pp. 13-32.

Radivojević, M. 2015. Inventing metallurgy in western Eurasia: a look through the microscope lens. *Cambridge Archaeological Journal,* 25, pp. 321-338.

Radivojević, M. & Kuzmanović-Cvetković, J. 2014. Copper minerals and archaeometallurgical materials from the Vinča culture sites of Belovode and Pločnik: overview of the evidence and new data. *Starinar,* 64, pp. 7-30.

Radivojević, M. & Rehren, Th. 2016. Paint It Black: The Rise of Metallurgy in the Balkans. *Journal of Archaeological Method and Theory,* 23, pp. 200-237.

Radivojević, M., Rehren, Th., Kuzmanović-Cvetković, J., Jovanović, M. & Northover, J. P. 2013. Tainted ores and the rise of tin bronze metallurgy, c. 6500 years ago. *Antiquity,* 87, pp. 1030-1045.

Radivojević, M., Rehren, Th., Pernicka, E., Šljivar, D., Brauns, M. & Borić, D. 2010. On the origins of extractive metallurgy: new evidence from Europe. *Journal of Archaeological Science,* 37, pp. 2775-2787.

Rapp, G. 2009. *Archaeomineralogy,* Berlin, Heidelberg: Springer-Verlag.

Rehren, Th. 1997. Die Rolle des Kohlenstoffs in der Prähistorischen Metallurgie. *Stahl und Eisen,* 117, pp. 87-92.

Rehren, Th., Leshtakov, P. & Penkova, P. 2016. Reconstructing Chalcolithic copper smelting at Akladi cheiri, Chernomorets, Bulgaria *In:* Nikolov, V. & Schier, W. (eds.) *Der Schwarzmeerraum vom Neolithikum bis in die Früheisenzeit (6000-600 v.Chr.). Kulturelle Interferenzen in der zirkumpontischen Zone und Kontakte mit ihren Nachbargebieten.* Rahden/Westf.: Verlag Marie Leidorf GmbH.

Renfrew, C. 1969. The autonomy of the south-east European Copper Age. *Proceedings of the Prehistoric Society* 35, pp. 12-47.

Roberts, B. W., Thornton, C. P. & Pigott, V. C. 2009. Development of metallurgy in Eurasia. *Antiquity,* 83, pp. 1012-1022.

Seeliger, T. C., Pernicka, E., Wagner, G. A., Begemann, F., Schmitt-Strecker, S., Eibner, C., Öztunalı, Ö. & Baranyi, I. 1985. Archäometallurgische Untersuchungen in Nord- und Ostanatolien. *Jahrbuch des Römisch- Germanischen Zentralmuseums Mainz,* 32, pp. 597-659.

Sperl, G. 1990. Zur Urgeschichte des Bleies. *Zeitschrift für Metallkunde,* 81, pp. 799-801.

Sperl, G. 1991. Zur Geschichte der Verwendung des Bleies (Die Rolle des Bleies in der Geschichte der Metallurgie). *Jahrestagung des Arbeitskreises Archäometrie in der Fachgruppe Analytische Chemie der Gesellschaft Deutscher Chemiker (GDCH) und des Arbeitskreises Archäometrie und Denkmalpflege der Deutschen Mineralogischen Gesellschaft (DGM), 6.-8.3.1991, Berlin.* Berlin, pp. 47-51.

Stech, T. 1990. Neolithic Copper Metallurgy in Southwest Asia. *Archeomaterials,* 4, pp. 55-61.

Strahm, C. 1984. Die Anfänge der Metallurgie in Mitteleuropa. *Helvetica Archaeologica,* 97, pp. 1-39.

Thornton, C. P. 2001. The Domestication of Metal: A Reassessment of the Early Use of Copper Minerals and Metal in Anatolia and Southeastern Europe *(unpublished MPhil thesis).* Cambridge: University of Cambridge.

Thornton, C. P. 2009. The Emergence of complex metallurgy on the Iranian Plateau: escaping the Levantine Paradigm. *Journal of World Prehistory,* 22, pp. 301-327.

Thornton, C. P. 2014. The Emergence of Complex Metallurgy on the Iranian Plateau. *In:* Roberts, B. W. & Thornton, C. P. (eds.) *Archaeometallurgy in Global Perspective.* New York: Springer, pp. 665-696.

Twiss, K. C., Bogaard, A., Bogdan, D., Carter, T., Charles, M. P., Farid, S., Russell, N., Stevanović, M., Yalman, E. N. & Yeomans, L. 2008. Arson or Accident? The Burning of a Neolithic House at Çatalhöyük. *Journal of Field Archaeology,* 31, pp. 41-57.

Tylecote, R. F. 1976. *A History of Metallurgy,* London: The Metals Society.

Wagner, G. A., Begemann, F., Eibner, C., Lutz, J., Öztunali, Ö., Pernicka, E. & Schmitt-Strecker, S. 1989. Archäometallurgische Untersuchungen an Rohstoffquellen des frühen Kupfers in Ostanatoliens. *Jahrbuch des Römisch- Germanischen Zentralmuseums Mainz,* 36.

Wagner, G. A., Pernicka, E., Seeliger, T. C., Lorenz, I. B., Begemann, F., Schmitt-Strecker, S., Eibner, C. & Öztunali, Ö. 1986. Geochemische und isotopische Charakteristika früher Rohstoffquellen für Kupfer, Blei, Silber und Gold in der Türkei. *Jahrbuch des Römisch- Germanischen Zentralmuseums Mainz,* 33, pp. 723-730.

Wertime, T. A. 1964. Man's first encounters with metallurgy. *Science,* 146, pp. 1257-1267.

Yalçın, Ü. & Pernicka, E. 1999. Frühneolitische Metallurgie von Aşıklı Höyük. *In:* Hauptmann, A., Pernicka, E., Rehren, Th. & Yalçın, Ü. (eds.) *The Beginnings of Metallurgy, Der Anschnitt, Beiheft 9.* Bochum: Deutsches Bergbau-Museum, pp. 45-54.

Yener, K. A., Sayre, E. V., Joel, E. C., Özbal, H., Barnes, I. L. & Brill, R. H. 1991. Stable lead isotope studies of central taurus ore sources and related artifacts from eastern mediterranean chalcolithic and bronze age sites. *Journal of Archaeological Science,* 18, pp. 541-577.

Box (Section) No.	Description	Material characterisation	Publication
CH 5/88	Ore from Shrine A.VI.1		
CHM 1	**1 round block**	**Cu-based mineral**	
CHM 2	*2 halves of a large mineral (polished and unpolished)*	*Cu-based mineral*	
CH 2/88	Copper lumps from Grave 2 in E.VI.8		
CHM 3	**1 block**	**Cu-based mineral**	
CHM 4	**1 block**	**Cu-based mineral**	
CH 5/88	Ore lump from House E.VII.10		
CHM 5	**1 block**	**Cu-based mineral**	
CHM 6	*remaining fragment*	*Cu-based mineral*	
CH 2/88	Copper lumps with soil from House E.VII.10		
CHM 7	*1 Phial*	*Cu-based material*	
CHM 8	*1 Phial*	*Cu-based material*	
CH 6/88	House E.VI.1. Grave 5, Central Platform		
CHM 9	**1 Phial**	**Cu-based material**	
CHM 10	**1 block A**	**Cu-based material**	
CHM 11	**1 block B**	**copper slag'**	Neuninger et al. 1964
CHM 12	**1 Block C**	**Cu-based material**	
CH 1/88	Beads from the grave in the northern corner in Shrine A.VI.1		
CHM 13	**1 Phial**	**copper metal**	
CHM 14	**1 block**	**copper metal**	
CHM 15	**1 block (shared with large bead CHM 30)**	**copper metal**	
CHM 16	**1 can**	**copper metal**	
CH 4/88	Lead from Grave E.VI.29		
CHM 17	1 block, 7/1	galena	Sperl 1990
CHM 18	1 block, 7/2	galena	Sperl 1990
CHM 19	1 block, 7/4	galena	Sperl 1990
CHM 20	1 Phial /5	galena	Sperl 1990
CHM 21	1 Phial /6	galena	Sperl 1990
CHM 22	1 Phial /7	galena	Sperl 1990
CHM 23	1 Phial /8	galena	Sperl 1990
CHM 24	1 block, 7/3	galena	Sperl 1990
CHM 25	1 block	galena	Sperl 1990
CHM 26	1 block (Pb CH 13.6.80)	galena	Sperl 1990
CHM 27	**1 block (CH3393 27.8.87)**	**modern slag**	
CHM 28	1 free sample of lead?	galena?	
CH 1/88	Shrine E.VI.31, 2 beads from the burial		
CHM 29	*1 Phial*	*copper metal*	
CHM 30	**1 block (shared with beads CHM 15)**	**copper metal**	
CH 7/88	Level VI		"Pittioni 1963" (?)
CHM 31	**1 large block a**	**haematite**	
CHM 32	**1 large block b**	**haematite**	
CHM 33	**1 large block c**	**Cu-based material**	
CHM 34	**1 small block a**	**copper metal**	
CHM 35	**1 small block b**	**copper metal**	
CHM 36	1 Obsidian	obsidian	
CHM 37	a green object	bone in contact with malachite?	

Table 1: Çatalhöyük samples available for analyses from the Austrian collection (partially published in Neuninger et al. 1964). Please note that we were not able to locate reference "Pittioni 1963", written down next to the CH

Levels	No. of Shrine	(Mellaart 1967: 81, Tab. 13) 'metal'	Finds available for study from Neuninger et al. (Table 1)				
			Cu mineral	Galena	Metal	Slag (?)	Other
II	A.II.1	X					
IV	E.IV.8	X					
VI (B)	***E.VIB.1***	***X***	***3***			***1***	
VI (B)	***E.VIB.8***	***X***	***2***				
VI (B)	E.VIB.10	X					
VI (B)	E.VIB.12	X					
VI (B)	***E.?VIB.29***	***X***		***dozen beads***			***modern slag***
VI (A&B)	***E.VI.31***	***X***			***2 beads***		
VI (A&B)	***A.VI.1=E.VI.61=A.VI.61***	***X***	***2***		***dozen beads***		
VI	***un-provenanced***		***1 (2)***		***2***		***obsidian, haematite, bone fragment?***
VII	***E.VII.10***		***2 (1) + 4***				
VII	E.VII.35	X					
IX	E.IX.1	X					

Table 2: Table associating shrines with the presence/absence of metal finds (according to Mellaart 1967: 81, Tab. 13, presence marked with X) and number of samples available for study, separated by the material type: Cu mineral, galena, metal, slag (?) and other. Note that no material marked initially by Mellaart as 'metal' is available from Shrines A.II.1, E.IV.8, E.VI.B.10, E.VI.B.12, E.VII.35 and E.IX.1.

7/88, Level VI in the original documentation. Samples marked as **bold** were (re)analysed, while samples in italic (CHM 2, 6-8, 29) were characterised only macroscopically.

	Al	Si	S	K	Ca	Fe	Cu	Zn	Sb	O
sample	at%	at%	at%	at%	at%	at%	at%	at%	at%	at%
CHM3	1.4	3.4	0.0	0.1	0.0	0.3	42.9	0.0	0.0	52.0
stdev.s	*0.9*	*1.5*	*0.0*	*0.2*	*0.0*	*0.6*	*3.1*	*0.0*	*0.0*	*0.7*
CHM4	1.6	7.5	0.8	0.1	0.2	0.7	34.2	0.0	0.0	54.9
stdev.s	*1.2*	*2.0*	*0.2*	*0.3*	*0.3*	*0.5*	*1.6*	*0.0*	*0.0*	*0.7*
CHM 9	0.0	0.0	0.0	0.0	0.0	0.0	49.5	0.4	0.1	50.0
stdev.s	*0.0*	*0.0*	*0.0*	*0.0*	*0.1*	*0.0*	*0.6*	*0.5*	*0.2*	*0.1*
CHM10	0.0	0.0	0.0	0.0	0.1	0.0	48.8	1.1	0.0	50.0
stdev.s	*0.0*	*0.0*	*0.0*	*0.0*	*0.2*	*0.0*	*1.5*	*1.5*	*0.0*	*0.0*
CHM 33	0.0	0.0	0.0	0.0	0.0	0.0	55.0	0.0	0.0	45.0
stdev.s	*0.0*	*0.0*	*0.0*	*0.0*	*0.0*	*0.0*	*7.5*	*0.0*	*0.0*	*7.5*

Table 3: SEM-EDS compositional data for green phases in copper-based minerals from Çatalhöyük, normalised to 100%. As and Pb values were below the detection limit of 0.1 wt%. All values are given as stoichiometrically calculated at% averages and sample standard deviation.

	Si	Ca	Mn	Fe	Cu	Zn	As	Sb	Pb	O
sample	at%	at%	at%	at%	at%	at%	at%	at%	at%	at%
CHM 9	2.8	9.1	0.0	0.9	2.0	0.0	0.0	22.8	5.4	57.1
stdev.s	*0.0*	*0.2*	*0.0*	*0.1*	*0.8*	*0.0*	*0.0*	*0.4*	*0.1*	*0.1*
CHM 10	0.9	3.8	0.0	0.9	16.7	0.5	9.8	6.6	6.3	54.5
stdev.s	*0.8*	*1.0*	*0.0*	*0.4*	*2.2*	*0.8*	*2.7*	*4.0*	*0.9*	*0.7*

Table 4: SEM-EDS compositional data for white/bright phases in copper-based minerals CHM 9 and CHM 10 from Çatalhöyük, normalised to 100%. All values are given as stoichiometrically calculated at% averages and sample standard deviation.

	Si	Ca	Fe	Cu	Zn	As	Sb	O
	at%	at%	at%	at%	at%	at%	at%	at%
CHM1 dark grey	0.0	0.2	0.3	46.1	0.3	2.5	0.0	50.6
stdev.s	*0.0*	*0.2*	*0.3*	*4.5*	*0.5*	*2.9*	*0.0*	*0.7*
CHM 1/5 light grey	0.2	0.4	0.2	24.4	5.5	14.2	1.1	53.9
stdev.s	*0.4*	*0.7*	*0.4*	*1.6*	*1.0*	*1.0*	*1.2*	*0.2*

Table 5: SEM-EDS compositional data dark (CHM 1) and light phases in CHM 1 and CHM 5, normalised to 100%. All values are given as stoichiometrically calculated at% averages and sample standard deviation.

	S	Fe	Cu	Zn	As	Sb
	at%	at%	at%	at%	at%	at%
CHM 1	45.5	3.2	34.2	3.2	5.0	8.9
stdev.s	*0.3*	*0.2*	*0.4*	*0.2*	*0.2*	*0.2*
CHM 5	45.3	2.0	35.1	3.6	5.4	8.7
stdev.s	*0.3*	*0.1*	*0.2*	*0.2*	*0.2*	*0.2*

Table 6: SEM-EDS compositional data for pale/white phases in CHM 1 and CHM 5, normalised to 100%. All values are given as at% averages and sample standard deviation.

	Na2O	MgO	Al2O3	SiO2	P2O5	SO3	K2O	CaO	TiO2	MnO	FeO	CuO	ZnO	PbO
	wt%	wt%	wt%	wt%	wt%	wt%	wt%	wt%	wt%	wt%	wt%	wt%	wt%	wt%
loc 5	1.3	5.9	2.9	45.5	2.2	0.0	0.6	23.4	0.0	0.0	2.8	8.2	6.9	0.4
stdev.s	*1.2*	*1.1*	*0.8*	*8.5*	*0.5*	*0.0*	*0.2*	*4.0*	*0.0*	*0.0*	*0.8*	*3.8*	*1.6*	*0.7*
loc 8	2.6	2.3	12.4	50.2	1.3	0.0	2.8	6.0	1.0	0.0	10.3	11.0	0.0	0.0
stdev.s	*0.2*	*0.5*	*0.9*	*9.4*	*0.5*	*0.0*	*0.5*	*2.5*	*0.2*	*0.0*	*6.3*	*2.5*	*0.0*	*0.0*
loc 11	0.7	2.2	8.0	45.8	3.7	0.3	1.7	4.8	0.1	0.0	26.2	6.5	0.0	0.0
stdev.s	*1.0*	*0.5*	*2.0*	*15.1*	*1.2*	*0.7*	*0.3*	*1.0*	*0.2*	*0.0*	*10.5*	*1.9*	*0.0*	*0.0*

Table 7: SEM-EDS compositional data for bulk slag analyses in areas varying from c. areas varying in size from c. 50 x 50 microns to 100 x 100 microns in locations 5, 11, and 8 in CHM 11, normalised to 100%. As and Sb values were below the detection limit of 0.1 wt%. All values are given as averages and sample standard deviation.

	Na2O	MgO	Al2O3	SiO2	P2O5	SO3	K2O	CaO	TiO2	MnO	FeO	CuO	ZnO	PbO
	wt%	wt%	wt%	wt%	wt%	wt%	wt%	wt%	wt%	wt%	wt%	wt%	wt%	wt%
loc 5	0.4	5.7	3.6	45.3	2.9	0.0	0.7	23.0	0.0	0.0	3.4	7.6	7.4	0.1
stdev.s	*0.8*	*0.9*	*0.8*	*2.1*	*0.7*	*0.0*	*0.2*	*4.5*	*0.0*	*0.0*	*0.8*	*3.2*	*0.9*	*0.3*
loc 8	0.6	2.9	13.6	48.7	1.4	0.1	3.0	6.8	1.1	0.0	8.8	12.7	0.0	0.4
stdev.s	*1.0*	*0.5*	*5.1*	*4.2*	*0.6*	*0.3*	*0.7*	*2.2*	*0.5*	*0.0*	*3.3*	*3.3*	*0.0*	*0.6*
loc 11	1.2	3.1	11.8	39.0	5.1	0.0	2.1	6.2	0.5	0.0	29.8	1.2	0.0	0.0
stdev.s	*0.3*	*0.3*	*1.3*	*0.8*	*0.6*	*0.0*	*0.4*	*0.5*	*0.1*	*0.0*	*2.3*	*0.4*	*0.0*	*0.0*

Table 8: SEM-EDS compositional data (spot analyses) for the glassy slag matrix in CHM 11 (locations 5, 8 and 11), all normalised to 100%. As and Sb values were below the detection limit of 0.1 wt%. All values are given as averages and sample standard deviation.

	Mg	Al	Si	P	S	K	Ca	Fe	Cu	O
	at%	at%	at%	at%	at%	at%	at%	at%	at%	at%
location 8 delaf	0.0	2.7	0.0	0.3	0.0	0.1	0.2	23.5	22.2	50.9
stdev.s	*0.0*	*0.6*	*0.0*	*0.4*	*0.0*	*0.1*	*0.3*	*0.9*	*1.7*	*0.4*
location 11 delaf	0.0	1.9	0.3	0.0	0.4	0.0	0.8	21.8	23.8	51.0
stdev.s	*0.0*	*0.1*	*0.4*	*0.0*	*0.0*	*0.0*	*0.6*	*1.5*	*0.3*	*0.2*
location 11 spinel	0.6	1.9	4.4	1.0	0.1	0.3	1.3	34.6	2.6	53.4
stdev.s	*0.6*	*0.7*	*2.9*	*0.2*	*0.1*	*0.2*	*0.6*	*6.5*	*1.3*	*1.4*
location 15 spinel	0.0	2.1	0.8	0.3	0.0	0.0	0.1	30.7	14.7	51.2
stdev.s	*0.0*	*1.9*	*0.7*	*0.3*	*0.0*	*0.0*	*0.1*	*2.2*	*2.1*	*1.0*

Table 9: SEM-EDS compositional data for delafossite in locations 8, 11 and iron spinels in locations 11 and 15 in CHM 11. All values are given as stoichiometrically calculated at% averages and sample standard deviation.

		Mg	Al	Si	P	Mn	Fe	Co	Ni	Cu	Zn	As	Se	Ag	Cd	Sn	Sb	Te	Au	Pb	Bi
Lab-ID	**mLoD**	**1**	**13**	**300**	**70**	**3**	**60**	**0.6**	**22**	**6**	**2**	**3**	**10**	**2**	**0.4**	**1**	**0.2**	**0.8**	**1**	**1**	**0.04**
MA-152378	CHM 11	<LoD	<LoD	<LoD	<LoD	<LoD	<LoD	<LoD	250	992000	6	1400	15	17	<LoD	<LoD	6100	<LoD	<LoD	58	1.84
MA-152380	CHM 15_30	<LoD	<LoD	195	<LoD	<LoD	<LoD	<LoD	<LoD	1000000	<LoD	24	<LoD	320	<LoD	<LoD	<LoD	<LoD	<LoD	<LoD	<LoD

Table 10: LA-ICP-MS compositional data for copper metal phases in CHM 11 (location 5) and CHM 15 (this sample is in the same resin block as CHM 30, hence the label). All values are given in µg/g.

	O	S	Ca	Fe	Cu	Zn	As	Sb	Pb
	at%	at%	at%	at%	at%	at%	at%	at%	at%
light grey	3.8	0.5	0.0	0.0	70.0	0.0	0.3	24.7	0.7
stdev.s	*1.3*	*0.5*	*0.0*	*0.0*	*2.3*	*0.0*	*0.4*	*1.1*	*0.7*
grey	4.2	0.0	0.0	0.0	55.1	0.0	0.0	26.2	14.5
stdev.s	*1.5*	*0.0*	*0.0*	*0.0*	*7.0*	*0.0*	*0.0*	*2.9*	*4.8*

Table 11: SEM-EDS compositional data for optically pale metal prills with light grey and grey eutectic in the middle of location 5, sample CHM 11 (see Fig. 13g). All values are given as at% averages and sample standard deviation.

Lab no.	Original ID	$^{208}Pb/^{206}Pb$ mean	$^{208}Pb/^{206}Pb$ 2σ	$^{207}Pb/^{206}Pb$ mean	$^{207}Pb/^{206}Pb$ 2σ	$^{208}Pb/^{204}Pb$ mean	$^{208}Pb/^{204}Pb$ 2σ	$^{207}Pb/^{204}Pb$ calc mean	$^{207}Pb/^{204}Pb$ calc 2σ	$^{206}Pb/^{204}Pb$ calc mean	$^{206}Pb/^{204}Pb$ calc 2σ
MA-161935	CHM 13	2.0803	0.0001	0.84255	0.00001	18.620	0.001	38.735	0.006	15.688	0.001
MA-161936	CHM 16	2.0781	0.0001	0.84187	0.00001	18.636	0.001	38.726	0.006	15.689	0.001

Table 12: Lead isotope ratios of copper metal beads CHM 13 and CHM 16.

Repealing the Çatalhöyük extractive metallurgy:
The green, the fire and the 'slag'

Supplementary Materials

Miljana Radivojević[1*], Thilo Rehren[2*], Shahina Farid[2], Ernst Pernicka[3] & Duygu Camurcuoğlu[4]

[1]McDonald Institute for Archaeological Research, University of Cambridge, Cambridge, UK; mr664@cam.ac.uk
[2]UCL Institute of Archaeology, London, UK; th.rehren@ucl.ac.uk; and College of Humanities and Social Sciences, HBKU, Doha, Qatar
[3]Curt Engelhorn Zentrum Archaeometrie, Mannheim, Germany
[4]Department of Conservation, The British Museum, London, UK

*corresponding authors

Supplementary text

Introduction to the site

James Mellaart began excavations at Çatalhöyük in 1961 (Mellaart, 1962). Prior to this, he had already taken part in several excavations (Balter, 2005: 18), as well as directing his own excavations at Chalcolithic Hacilar (Mellaart, 1960), which enhanced interpretations of the development of early urban settlements, the appearance of domesticated plants and animals, and the accompanying material culture that these discoveries entailed. Because of his survey work of the site in 1958 (Mellaart, 1961: 158), Mellaart had a foretaste for what to expect at Çatalhöyük and what it should unveil in terms of early pottery production, stone and lithic technology, symbolism and metallurgy. In his first preliminary report Mellaart (1962: 41) states: "*As Hacilar showed a gap in its culture sequence exactly during the Early Neolithic period, which finds showed was best represented at Çatal Hüyük, it was decided to start excavations at this site to complete the sequence and throw further light on Hacılar*".

Mellaart defined two types of buildings: 'shrines' and 'houses'. These were differentiated by several factors: shrines were identified by the 'richness' of decoration; the presence of wall-paintings of an elaborate nature that have apparent ritual or religious significance; plaster reliefs showing deities, animals or animal heads; horns of cattle set into benches; rows of bucrania and groups of cult statues found in the main room; ex-voto figures stuck into the walls; human skulls set up on platforms, etc. According to Mellaart (1967: 78), all these features do not occur in 'normal' houses and the combination of several of these factors is taken as leaving *"little doubt that the building in which they are found was used as a cult room or shrine*"

Excavations and research conducted under the directorship of Ian Hodder (1993 - current) reviewed these distinctions and led to a preference for a non-hierarchical classification of 'building', which will be used here. This was based on the criteria that the internal plan and furnishing of all buildings indicated a uniformly domestic function. The criteria that Mellaart had defined were not incorrect but demonstrably all buildings contain a degree of elaboration. Current studies, drawn on statistical variations in 'elaboration' to define architectural or social rank at the site, have introduced the concept of 'history houses' (Hodder and Pels, 2010) in place of 'shrines', thereby removing the presumed religious connotation but acknowledging distinctions that Mellaart had rationalised.

On fire in Level VI

Current discourse on burnt buildings from the renewed excavations centre around the debate of deliberate versus accidental burning of buildings (Cessford and Near, 2005; Twiss et al., 2008). So far, these attest to the clustering of burnt buildings around the Level VI horizon. The fires, however, appear to have occurred on a house-by-house basis and there is no clear evidence to resolve how they took to flame (Harrison et al., 2013; Farid, 2014: 393). The forensic fire examination of these burnt buildings conducted by Harrison et al. (2013) identified a range of mechanisms by which buildings burned at Çatalhöyük involving 'compartment' and 'combustion' fires, which depend on fuel load and thermal characteristics. Experimental work conducted to assess the ability to raise subsurface deposits to such temperatures that fully charred skeletal remains and, in some cases carbonised brain tissue, was undertaken on porcine brain tissue. It demonstrated that a temperature of c. 300 °C must be maintained over about a two-hour period for the brain tissue to be carbonised but to char bone 30 kg of timber was required to fuel a fire over an eight-hour period. The conclusion is that the duration of burning was the dominant variable in producing carbonisation rather than the peak temperature achieved.

Chronology of the metallurgical finds

Since the first excavations on the site, the twin planks of chronology at Çatalhöyük have been the deep relative sequence provided by archaeological stratigraphy and radiocarbon dating. Combining these two strands of information to provide a calendar timescale for the mound has always been a central objective for research on the site. Between 1963 and 1968 Mellaart obtained 27 radiocarbon dates from the University of Pennsylvania radiocarbon laboratory (Stuckenrath and Ralph, 1965; Stuckenrath and Lawn, 1969). Eight of these measurements come from buildings that contained metallurgical finds.

Arising from further excavations in Mellaart's Area E in the 1990s, 42 AMS measurements were obtained and a Bayesian model constructed for Mellaart's sequence of Levels (Göktürk et al., 2002; Cessford, 2005). Although 23 of these measurements came from new excavations on the remnants of buildings and courtyards recorded by Mellaart, only the wiggle-match sequence from a charred juniper post in E.IV.1 is relevant to this study. This timber formed part of a 577-ring floating tree-ring chronology (Kuniholm and Newton, 1996; Newton and Kuniholm, 1999;

Cessford, 2005: 79-81) that contained timbers from two buildings that contained metallurgical finds.

A new programme of radiocarbon dating and Bayesian modelling for the east mound at Çatalhöyük is currently underway. This is attempting to combine the stratigraphical sequence of buildings and open areas with a large series of carefully selected radiocarbon dates, from both the current excavations and the 1960s archive. The stratigraphic analysis has been immeasurably aided by the addition of 27 large-scale original plans of the 1960s excavations, kindly provided by James Mellaart before his death. Both the radiocarbon dating and stratigraphic programmes are on-going and only partially reported (Bayliss et al., 2015; Marciniak et al., 2015), but so far this project has obtained radiocarbon dates for four buildings from which Mellaart reports metallurgical finds and has stratigraphic evidence allowing seven to be included in the working Bayesian chronological model.

Radiocarbon dates quoted in normal type in this paper have been calibrated using the maximum intercept method (Stuiver and Reimer, 1986); ranges in *italics* are formal Highest Posterior Density intervals from the recalculation of the wiggle-match presented by Cessford (2005) using IntCal13; dates cited in italics as *'circa'* or as '*centuries cal BC*' are tentative date estimates derived from the interim modelling of the east mound sequence. This is based both on an incomplete suite of radiocarbon dates and incomplete stratigraphic analysis, and so informal date estimates have been provided to avoid over-interpretation at this stage of research. All calculations have been undertaken using IntCal13 (Reimer et al., 2013) and OxCal v4.2 (Bronk Ramsey, 2009)

Five buildings with metallurgical finds currently have no radiocarbon dates. E.VII.35 is a stratigraphically isolated building that was on the surface of the mound. E.VI.5 was also on the surface, but is later than E.VII.5 (partially excavated and recorded between 1995 and 2002 as Sp.169) (Farid, 2007b: 325-326). E.VI.31 and E.IV.8 form part of a superimposed stack of six buildings, neither is dated, but E.IV.8 is later than E.VI.31 with E.V.8 in between. E.VIB.12 is part of a superimposed stack of four buildings and an open area. It is earlier than E.VIA.12, which was on the surface and is currently undated, and later than E.VII.12. The remnants of this building were investigated in 1995 and 1998 (as B.40) (Farid, 2007b: 313-320), demonstrating that in the earlier part of its occupation it was joined to E.VII.2 by an access hole. This building

in turn, was later than court E.VIII.12 (investigated as Sp.115). The preliminary model from the new dating programme currently suggests a *terminus post quem* of *c. 6600 cal BC* for E.VIB.12.

A bulk sample of charred grain from bin or hearth in building A.II.1 produced a date of 6490–6230 cal BC (at 2σ, P-796, 7521±77 BP), and a sample of charred human brain from skeleton 3 in building E.VI.1, which was 'found under central platform where stratification of skeletons indicates that this burial was rather early in the sequence found there' and was accompanied by a necklace of black beads (Stuckenrath and Ralph, 1965: 192), provides a date of 6600–6240 cal BC (at 2σ, P-827, 7579±89 BP). The grave containing 'many fragments of a string-skirt the ends of which appear to have been encased in thin copper tituli to weight it down' (Mellaart, 1963: 101) was discovered in 1962 and therefore came from E.VIA.25. A sample of carbonised grain from this building has been dated to 6510–6240 cal BC (at 2σ; P-769, 7505±93 BP).

Three further measurements come from charred timbers, two of which have been incorporated in the floating tree-ring ring sequence produced by dendrochronology, which is currently dated by radiocarbon wiggle matching. One of these, a juniper roof beam from A.VI.1 (previously dated by P-770, 7912±94 BP), was complete to bark and so was felled in *6515–6435 cal BC (95% probability; CTL-6*) (cf. Cessford, 2005: Fig. 4.4). This is compatible with a date of 6560–6220 cal BC (at 2σ; P-781, 7525±90 BP) from an oak roof beam from the same building. The possibility that the timber was reused in A.VI.1 cannot, of course, be dismissed. A juniper post from E.VIB.10 (previous dated by P-777, 7704±91 BP) was missing an unknown number of rings and so thus felled after *6605–6525 cal BC* (*95% probability; CTL13&14*) (cf. Cessford, 2005: Fig. 4.4).

This date for E.VIB.10 is compatible with a new series of measurements from human burials and articulating animal bone from E.VII.10 beneath (the remnants of this building were excavated as B.24 in 1998) (Farid, 2007b: 330-337). These suggest that the use of this building *centered on the 67th century cal BC*, perhaps suggesting that CTL13&14 from the succeeding building had not lost many rings before sampling and came from a freshly felled timber. E.IX.1 and E.VIB.8 also appear in the new dating programme. Excavations in 1999 demonstrated that E.IX.1 (B.22) was one build with E.IX.8 (B.16) and recorded a small area of surviving deposits in the latter (Farid, 2007a). This building is securely stratified in a column of six buildings recorded by Mellaart (the second of which is E.VIB.8), which can in turn be related to the 1999 deep

sounding (Bayliss et al., 2015) and a series of overlying middens (Regan, 2014). Preliminary modelling from the new dating programme suggests that use of E.IX.1 *centred on the 68th century cal BC* (the existing result (P-779, 8190±99 BP) either being from the centre of a long-lived tree or from a reused timber), and that E.VIB.8 was used *in the latter part of the 67th century cal BC*. Some radiocarbon results are now also available from the sequence of eight buildings and open areas that include E.VI.29, all from material surviving in the 1960s archive. Preliminary modellings suggests that E.VI.29 may have been in use *in the generations around 6600 cal BC.*

A summary of the chronology of the dated buildings with metallurgical finds is provided in Figure 4 in the main text. It is clear that Level VI does not form a concentrated chronological horizon. A.VI.1, for example, appears to be about a century later than E.VIB.8 and E.VIB.29, and overall buildings assigned to Level VI appear to fall anywhere between the 67th and 64th centuries cal BC. On currently evidence, it appears that metallurgical finds occur at Çatalhöyük across most of the seventh millennium cal BC.

Characterisation of materials

All samples were received as mostly polished blocks (with one to several samples embedded in each epoxy resin blocks, see for example Fig. 3), several phials and a can with a dozen mineral and metal beads, as well as freestanding samples with or without plastic bags. They were packed in four customised boxes (Fig. S1), the lids of which were marked with red pen delineating sections labelled with CH 1/88 to CH 7/88 and accompanied with a document explaining the content of the boxes and related enumerations (see also Table 1). We re-polished the already prepared samples in epoxy resin (twenty two blocks, some re-mounted) and made one new block from a sample coming from the 'pyrometallurgical' batch (CHM 9 as newly mounted in addition to already mounted CHM 10-12, see Table 1).

On modern slag piece (CHM 27)

Noteworthy is the sample of an ***industrial slag*** labelled here as CHM 27 (Fig. 5 in the main text). Although it came with the Çatalhöyük material, we concluded that it probably ended up in this collection by mistake. The first indication was the label; it revealed the date (27.8.87) different from the sample that certainly belonged to the Çatalhöyük project (Pb CH 13.6.80). Also, the

first part of the label of an industrial slag piece being CH(3393) could have confused a person that dealt with the materials stored for almost 50 years in the Institute for Prehistory and Historical Archaeology at the University of Vienna in Austria. Furthermore, compositional analyses done by SEM-EDS revealed ferrosilicon droplets suspended in a glass matrix made of iron alumina silicates. Ferrosilicons with the content of c. 45 wt% in CHM 27 are known to be made in modern electric arc furnaces, which makes them an unlikely find from c. 8500 years ago.

Figure S1: Four double-layered accustomed boxes of Çatalhöyük materials as they reached the UCL Institute of Archaeology in 2010.

Methodology

Sampling and Preparation

The research collection was appropriately catalogued, measured and photographed prior to sample preparation and analysis. This stage was followed by a careful designing of analytical strategy for each sample.

We decided to either re-polish or re-cast the 'old' blocks with Çatalhöyük samples and later include any additional samples that we deem important for further inspection. The only sample

that we freshly made was CHM 9, which came from the batch of samples indicative of high-temperature treatment. We initially tested all five samples belonging to the pack we labelled as CHM 9 for magnetic properties, and upon finding that none of them was responsive, we chose the largest item from the assemblage for casting in epoxy resin.

Samples selected for further microstructural and compositional study were ground using abrasive disks (1200, 2400 and 4000 grit) and polished using diamond pastes (1 μm and ¼ μm). Mounted polished blocks were washed in an ultrasonic bath and rinsed with ethanol between each polishing stage. As polished blocks they were suitable for the initial analytical stage, reflected light microscopy (OM), with photomicrographs taken on the Leica and Olympus microscopes at 25x, 50x, 100x, 200x, 500x and 1000x. In the following analytical stage, compositional analysis, samples were carbon-coated to be suitable for examination under the Scanning Electron Microscope with Energy Dispersive Spectrometer (SEM-EDS). Both preparation and OM and SEM-EDS analyses were conducted at the Wolfson Archaeological Science Laboratories, UCL Institute of Archaeology, London.

Microstructural Analysis

Analyses of microstructures were conducted primarily with optical microscopy (OM), while SEM-EDS played only a minor role in distinguishing phases in the studied samples. Optical microscopy is an established method in archaeometallurgy for studying optical properties of geologically-formed minerals (e.g. oolithic formations) or artificially generated phases (e.g. crystals in the slag matrix). These properties were used to identify which minerals/phases were present in the sample and inform on their generation. OM analyses were conducted on all polished blocks, Leica DMLM microscope (Table S1).

Compositional Analysis

SEM-EDS

SEM-EDS was used to chemically characterise the phases present in the samples and assess their relation to the given analytical context (Table S1). It was applied for analysing all types of materials mounted in polished blocks. All polished blocks were carbon-coated, and analysed under the same conditions: accelerating voltage of EDS was 20 kV, with an average deadtime of 35-40% and working distance of 10 mm. The analytical volume of the beam varied depending on

the density of the analysed material. For metallic phases, its diameter is in the range of 2 μm, while for lighter phases/materials such as slag or ceramic, it is nearer 5 μm. BSE imaging was used as default for faster recognition of samples' components. The data processing was controlled by INCA X-cite software, which processes, displays and stores the images and spectra acquired by the analyser. Cobalt standard is used to calibrate the EDS analyser, which was scanned at the beginning of each session to guard against analytical drift. The acquired spectra from all analysed samples were carefully checked for every detected element, and particularly visually searched for the following elements: Mn, Fe, Co, Ni, Cu, Zn, As, Sn, Sb, and Pb.

Provenance analysis

MC-ICP-MS

For the purpose of this research 4 samples in total were analysed for their lead isotope abundance ratios (Table S2) on the Multi-Collector Inductively-Coupled Plasma Mass Spectrometer (MC-ICP-MS), located at the Centre for Archaeometry in Mannheim. This instrument is a hybrid mass spectrometer with an advantage to analyse a broader range of elements than TIMS, commonly used in the past for lead isotope measurements. Its primary components are an ICP source (where ions are produced, accelerated, focused), an analyser (where ions are filtered to be separated based on their mass ratios), and a series of collectors (where the ion beams are measured simultaneously). The sample preparation and analyses were done according to the standard procedure explained in Niederschlag et al. (2003).

LA-ICP-MS

Laser Ablation Inductively-Coupled Plasma Mass Spectrometer was used for trace element analysis. The instrumentation was a Thermo X-Series II inductively- coupled plasma mass spectrometer coupled with a Resonetics laser ablation system (ArF, 193 nm). The parameters of the ICP-MS are optimized to ensure a stable signal with a maximum intensity over the full range of masses of the elements and to minimize the formation of oxides and double-ionized species. The diameter of the laser beam and thus the analyzed sample area was 100 μm. Quantification was carried out using ablation yield correction factors with normalization of the major components to 100 % (Kovacs et al., 2009).

Instruments	Aim of Analysis	Analytical Parameters
Reflected Polarized Light Microscopy (Leica DMLM)	Phase identification and visual characterisation of microstructure	Plane polarized light and crossed polarized light were applied to examine phases in samples, their colour, homogeneity, porosity and inclusions (shape, size and uniformity). Cross-polarized light was also applied for internal reflection and identifying the composition of phases present. The microscope was equipped with a Nikon digital camera, with the highest magnification of 1000x.
SEM-EDS Scanning Electron Microscopy with Energy Dispersive Spectrometry (Superprobe JEOL- JXA-8600)	1. Phase identification in samples using electron images and area/point analyses 2. Quantitative compositional analyses of observed phases 3. Observation of the relationships between phases on the basis of their atomic number contrast	Backscattered electron (BSE) imaging used. The accelerating voltage was 20 kV, with average dead-time of 35-40 % and working distance of 10 mm. The analytical volume of the beam depended on the density of analysed material, for metallic phases its diameter was c. 2 µm, and for lighter materials (ie. slag), nearer 5 µm. All data are presented as normalized with stoichiometrically added oxygen, if not otherwise stated. The iron content is presented as FeO, which here stands for total iron (both valencies).
ICP-MS Inductively Coupled Plasma Mass Spectrometry (Neptune Plus HR-MC-ICP-MS)	Lead isotope analysis	The samples were dissolved in diluted HNO_3 and lead was separated with ion chromatography resins from the matrix. Each sample was measured once, however in 3 runs.
LA ICP-MS Thermo X-Series II inductively- coupled plasma mass spectrometer coupled with a Resonetics laser ablation system (ArF, 193 nm)	Compositional analysis of copper metal phases in CHM 11 and CHM 15	Q-ICP-MS in time resolved mode; forward power 1400W, nebulizer gas (Ar) 0.8 l/min, cooling gas (Ar) 13 l/min. The diameter of the laser beam and thus the analyzed sample area was 50 µm. Laser settings: 8 mJ, repetition rate 5 Hz, helium gas flow 600 ml/sec. in.

Table S1: Analytical instruments used in this study, aim of analysis and relevant analytical parameters.

Label UCL	Material characterisation	polished block	OM	SEM	LIA	LA-ICP-MS
CHM1	Cu-based mineral	YES	X	X		
CHM2	*Cu-based mineral*					
CHM3	Cu-based mineral	YES	X	X		
CHM4	Cu-based mineral	YES	X	X		
CHM5	Cu-based mineral	YES	X	X		
CHM6	*Cu-based mineral*					
CHM7	*Cu-based material*					
CHM8	*Cu-based material*					
CHM9	Cu-based material	YES	X	X		
CHM10	Cu-based material	YES	X	X		
CHM11	copper slag'	YES	X	X		X
CHM12	Cu-based material	YES	X			
CHM13	copper metal	NO			X	
CHM14	copper metal	YES	X	X		
CHM15	copper metal	YES shared 15_30	X	X		X
CHM16	copper metal	NO			X	
CHM17	galena	YES	X	X		
CHM18	galena	YES	X	X		
CHM19	galena	YES	X	X		
CHM20	galena					
CHM21	galena				X	
CHM22	galena					
CHM23	galena					
CHM24	galena	YES	X	X		
CHM25	galena	YES	X	X		
CHM26	galena	YES	X	X		
CHM27	modern slag	YES	X	X		
CHM28	galena?					
CHM29	*copper metal*					
CHM30	copper metal	YES shared 15_30	X	X		
CHM31	haematite	YES	X	X		
CHM32	haematite	YES	X	X		
CHM33	Cu-based material	YES	X	X		
CHM34	copper metal	YES	X	X		
CHM35	copper metal	YES	X	X		
CHM36	obsidian					
CHM37	bone in contact with malachite?					

Table S2: Çatalhöyük materials presented in this study. Grey-shaded boxes indicate samples (re)analysed in this paper. Samples in italic were characterised macroscopically only.

Sample No.	Material	Year	Area	Unit	Context	Mellaart	Hodder	Colour	Paint id:
x19	Pigment	2003	4040	7575	Arbitary fill of burial [1202]. Found with beads and a bone tool.	Scrape	Scrape	Blue	Azurite
x1	Pigment	2003	4040	7597	Fill of burial cut	Scrape	Scrape	Blue	Azurite
x2	Pigment	2007	4040	16308	Burial, in situ. Blue pigment was found to the north of the skeleton. This pigment had a bone spatula sticking out of it and was surrounded by phytoltihs (perhaps a pouch).	n/a	Scrape G	Blue	Azurite
x1	Pigment	2007	4040	16133	Sp.17, F3025sk. Cluster of grave goods with the skeleton 16309	n/a	Scrape G	Green	Malachite
s2	Pigment	2001	BACH	8151	In situ burial (B.3 sk.8115)	n/a	BAC H G?	Blue	Azurite
s3	Pigment	2006	4040	13416	B.67, Sp.292-Northwest corner of B.67. Demolition backfill of space 292 - building 67	n/a	4040 H	Blue	Azurite
s1	Pigment	1995	SOUTH	1007	Sp.168, F417 (burial) grave fill. Mellaart shrine 6	Level VII	SOUT H M?	Green/ Blue	Azurite

Table S3: Contextual information for seven burial-related evidence for deposition of green (malachite, $Cu_2CO_3(OH)_2$) or blue (azurite, $Cu_3(CO_3)_2(OH)_2$) pigments in Çatalhöyük.

Material	Area	Unit	Feature	Reliability	Level	metal
Cu-based fragments (2 frag)	4040/North	7575.X17	unstratified – surface eroded Neolithic burial	Unstratified	II-IV Level allocation based on multiple evidential datasets	Yes
Context. *Multiple inhumation burial. "The fills within the burial feature contained numerous artefacts that could not be associated with an individual skeleton. The upper and lower fills ((7512) and (7575) respectively) were divided arbitrarily in order to provide horizontal control over the fill deposit. The lower fill contained numerous stone beads, a bone hairpin 7575.x16, an interlocking bone bead, copper beads 75755.x17 and some shell beads" (Yeomans, 2014).*						
Ring (2 frag)	TP	13079.X3	B.62/B.73	Residual	II/III	Yes
Context *Infill between two building sequences*						
Ring (complete)	South	16248.X1	Sp.427	Residual	V-VI	Yes
Context. *Midden. "The oven in Sp.333 now appears to have gone out of use and the area is subject to some midden dumping. These deposits broadly in sequence from earliest to latest are (16261) (16232) (16201), (15791), (16249) and (16248). All of this material yielded occasional charcoal, bone, pot and obsidian and also contained occasional ash lenses. Some of the more obvious interfaces between deposits may also have served as trodden surfaces but on the whole the build-up should be regarded as a continual process of deposition." (Regan, 2014).*						

Table S4: Contextual information for five copper fragments from the recent excavations at Çatalhöyük published by Birch et al. (2013).

Bibliography

Balter, M. 2005. *The Goddess and the Bull -Çatalhöyük: An Archaeological Journey to the Dawn of Civilization,* New York: Free Press.

Bayliss, A., Brock, F., Farid, S., Hodder, I., Southon, J. & Taylor, R. E. 2015. Getting to the Bottom of It All: A Bayesian Approach to Dating the Start of Çatalhöyük. *Journal of World Prehistory,* 28, pp. 1-26.

Birch, T., Rehren, Th. & Pernicka, E. 2013. The Metallic Finds from Çatalhöyük: A Review and Preliminary New Work. *In:* Hodder, I. (ed.) *Substantive Technologies at Çatalhöyük.* London, Los Angeles: British Institute at Ankara, Cotsen Institute of Archaeology, pp. 307-316.

Bronk Ramsey, C. 2009. Bayesian analysis of radiocarbon dates. *Radiocarbon,* 51, pp. 337-360.

Cessford, C. 2005. Absolute dating at Çatal Höyük. *In:* Hodder, I. (ed.) *Changing Materialities at Çatalhöyük: reports from the 1995-99 seasons.* Cambridge: McDonald Institute Monographs, British Institute at Ankara, pp. 65-100.

Cessford, C. & Near, J. 2005. Fire, burning and pyrotechnology at Çatalhöyük *In:* Hodder, I. (ed.) *Çatalhöyük perspectives: themes from the 1995-99 seasons.* Cambridge, London: McDonald Institute Monographs, British Institute of Archaeology at Ankara Monograph, pp. 171-182.

Farid, S. 2007a. Level IX. *In:* Hodder, I. (ed.) *Excavating Çatalhöyük: South, North and KOPAL Area reports from the 1995-99 seasons.* McDonald Institute Monographs, British Institute of Archaeology at Ankara Monograph: Cambridge, London, pp. 126-139.

Farid, S. 2007b. Level VII. *In:* Hodder, I. (ed.) *Excavating Çatalhöyük: South, North and KOPAL Area reports from the 1995-99 seasons.* Cambridge, London: McDonald Institute Monographs, British Institute of Archaeology at Ankara Monograph, pp. 283-338.

Farid, S. 2014. Building 52/51. *In:* Hodder, I. (ed.) *Çatalhöyük excavations: the 2000-2008 seasons.* London, Los Angeles: British Institute of Archaeology at Ankara Monograph, Cotsen Institute of Archaeology Press, pp. 357-397.

Göktürk, E. H., Hillegonds, D. J., Lipschutz, M. E. & Hodder, I. 2002. Accelerator mass spectrometry dating at Çatalhöyük. *Radiochimica Acta,* 90, pp. 407-410.

Harrison, K., Martin, V. & Webster, B. 2013. Structural fires at Çatalhöyük *In:* Hodder, I. (ed.) *Substantive Technologies at Çatalhöyük: Reports from the 2000-2008 Seasons.* London, Los Angeles: British Institute of Archaeology at Ankara Monograph, Cotsen Institute of Archaeology Press, pp. 137-146.

Hodder, I. & Pels, P. 2010. History houses. *In:* Hodder, I. (ed.) *Religion in the Emergence of Civilization.* Cambridge: Cambridge University Press, pp. 163-186.

Kovacs, R., Schlosser, S., Staub, S. P., Schmiderer, A., Pernicka, E. & Gunther, D. 2009. Characterization of calibration materials for trace element analysis and fingerprint studies of gold using LA-ICP-MS. *Journal of Analytical Atomic Spectrometry,* 24, pp. 476-483.

Kuniholm, P. & Newton, M. 1996. Interim Dendrochronological Progress Report 1995/6. *In:* Hodder, I. (ed.) *On the surface: Çatalhöyük 1993–95.* Cambridge: McDonald Institute for Archaeological Research and British Institute of Archaeology at Ankara, pp. 345-347.

Marciniak, A., Barański, M. Z., Bayliss, A., Czerniak, L., Goslar, T., Southon, J. & Taylor, R. E. 2015. Fragmenting Times: interpreting a Bayesian chronology for the late Neolithic occupation of Çatalhöyük East, Turkey. *Antiquity,* 89, pp. 154-176.

Mellaart, J. 1960. Excavations at Haçilar: third preliminary report 1959. *Anatolian Studies,* 10, pp. 83-104.

Mellaart, J. 1961. Early Cultures of the South Anatolian Plateau. *Anatolian Studies,* 11, pp. 159-184.

Mellaart, J. 1962. Excavations at Çatalhöyük: first preliminary report, 1961. *Anatolian Studies,* 12, pp. 41-65.

Mellaart, J. 1963. Excavations at Çatalhöyük, 1962: second preliminary report. *Anatolian Studies,* 13, pp. 43-103.

Mellaart, J. 1967. *Çatalhöyük, A Neolithic Town in Anatolia,* London: Thames and Hudson.

Newton, M. W. & Kuniholm, P. I. 1999. Wiggles worth watching – marking radiocarbon work. The case of Çatal Höyük. *In:* Betancourt, P. P., Karageorghis, V., Laffineur, R. & Niemeier, W. D. (eds.) *Meletemata: studies in Aegean archaeology presented to Malcolm H Weiner as he enters his 65th year. Aegeum 20.* Liège: Université de Liège, pp. 527-537.

Niederschlag, E., Pernicka, E., Seifert, T. & Bartelheim, M. 2003. The determination of lead isotope ratios by multiple collector ICP-MS: A case study of Early Bronze Age artefacts and their possible relation with ore deposits of the Erzgebirge. *Archaeometry,* 45, pp. 61-100.

Regan, R. 2014. The sequence of Buildings 75, 65, 56, 69, 44 and 10 and external Spaces 119, 129, 130, 144, 299, 314, 319, 329, 333, 339, 367, 371 and 427 with contributions by Taylor. *In:* Hodder, I. (ed.) *Çatalhöyük excavations: the 2000-2008 seasons.* London, Los Angeles: British Institute of Archaeology at Ankara Monograph, Cotsen Institute of Archaeology Press, pp. 131-190.

Reimer, P. J., Bard, E., Bayliss, A., Beck, J. W., Blackwell, P., Bronk Ramsey, C., Buck, C. E., Cheng, H., Edwards, R. L., Friedrich, M., Grootes, P. M., Guilderson, T. P., Haflidason, H., Hajdas, I., Hatté, C., Heaton, T. J., Hoffmann, D. L., Hogg, A. G., Hughen, K. A., Kaiser, K. F., Kromer, B., Manning, S. W., Niu, M., Reimer, R. W., Richards, D. A., Scott, E. M., Southon, J. R., Staff, R. A., Turney, C. S. M. & van der Plicht, J. 2013.

IntCal13 and Marine13 radiocarbon age calibration curves 0–50,000 years cal BP. *Radiocarbon,* 55, pp. 1869-1887.

Stuckenrath, R. & Lawn, B. 1969. University of Pennsylvania radiocarbon dates XI. *Radiocarbon,* 11, pp. 150-162.

Stuckenrath, R. & Ralph, E. K. 1965. University of Pennsylvania radiocarbon dates VIII. *Radiocarbon,* 7, pp. 187-199.

Stuiver, M. & Reimer, P. J. 1986. A computer program for radiocarbon age calculation. *Radiocarbon,* 28.

Twiss, K. C., Bogaard, A., Bogdan, D., Carter, T., Charles, M. P., Farid, S., Russell, N., Stevanović, M., Yalman, E. N. & Yeomans, L. 2008. Arson or Accident? The Burning of a Neolithic House at Çatalhöyük. *Journal of Field Archaeology,* 31, pp. 41-57.

Yeomans, L. 2014. Eroded Neolithic burials, Space 1003 *In:* Hodder, I. (ed.) *Çatalhöyük excavations: the 2000-2008 seasons.* London, Los Angeles: British Institute of Archaeology at Ankara Monograph, Cotsen Institute of Archaeology Press, pp. 547-556.